

The Gauge Theory of Measurement-Based Quantum Computation

Gabriel Wong,^a Robert Raussendorf^{b,c} and Bartłomiej Czech^d

^a*Center for Mathematical Sciences and Applications, Harvard University, Cambridge, MA 02138, USA*

^b*Department of Physics and Astronomy, University of British Columbia, Vancouver, Canada*

^c*Stewart Blusson Quantum Matter Institute, University of British Columbia, Vancouver, Canada*

^d*Institute for Advanced Study, Tsinghua University, Beijing 100084, China*

ABSTRACT: Measurement-Based Quantum Computation (MBQC) is a model of quantum computation, which uses local measurements instead of unitary gates. Here we explain that the MBQC procedure has a fundamental basis in an underlying gauge theory. This perspective provides a theoretical foundation for global aspects of MBQC. The gauge symmetry reflects the freedom of formulating the same MBQC computation in different local reference frames. The main identifications between MBQC and gauge theory concepts are: (i) the computational output of MBQC is a holonomy of the gauge field, (ii) the adaption of measurement basis that remedies the inherent randomness of quantum measurements is effected by gauge transformations. The gauge theory of MBQC also plays a role in characterizing the entanglement structure of symmetry-protected topologically (SPT) ordered states, which are resources for MBQC. Our framework situates MBQC in a broader context of condensed matter and high energy theory.

Contents

1	Introduction	2
2	Review of measurement-based quantum computation	5
2.1	The one-dimensional cluster state	5
2.2	MBQC	10
2.2.1	Basic idea	10
2.2.2	Measurement basis and temporal order	11
2.2.3	Computational output for MBQC on a chain	13
3	Preparations for the MBQC gauge theory	14
3.1	$\mathbb{Z}_2 \times \mathbb{Z}_2$ action and MPS tensor symmetries	14
3.2	Group labels for measurement outcomes	15
3.2.1	Incorporating temporal order	16
3.3	MBQC on a ring	18
4	The gauge theory of MBQC	20
4.1	Gauge principle	20
4.1.1	Formulating the MBQC gauge principle as a theorem	21
4.2	Mathematical underpinning of gauge theory	26
4.2.1	Fiber bundles, sections, and gauge transformations	26
4.2.2	Parallel transport	27
4.3	Holonomies and fluxes	30
4.4	Elements of computation	33
4.4.1	Output	33
4.4.2	Measurement basis from gauge fixing	34
5	Phenomenological ramifications of the gauge principle	35
5.1	Equivalent measurement records	35
5.2	MBQC holonomy and the virtual circuit simulation	36
5.3	Computational output and homotopy	37
5.4	A quantum MBQC gauge theory	38
5.4.1	Superselection (flux) sectors	39
5.4.2	A logical Hilbert space of fluxes	41
5.4.3	MBQC versus the circuit model	42
5.5	Extension to fixed point of SPT phases with onsite symmetries	43
5.6	Extension of the gauge principle to SPT cluster phase	44

1 Introduction

Measurement-based quantum computation (MBQC) [4] is a scheme of universal quantum computation driven solely by measurements; no unitary evolution takes place in the computational process. The measurements are local, and applied to an entangled initial state—the resource state. The resource perspective (see e.g. [5, 6], note [7], however) is suggested by the observation that once all the local measurements have been performed, the post-measurement state is a tensor-product state with no entanglement left. The initial entanglement has been converted into computational output. See Figure 1 for illustration.

The power of MBQC depends on the resource state used. Several types of resource states, such as cluster states [8] and AKLT states [9, 10] on various two-dimensional lattices, give rise to computational universality [4, 11–14]. On the other hand, some highly entangled states, such as Kitaev surface code states, have extremely limited computational power for MBQC [15]. As a general result, it is known that universal resource state are extremely rare in Hilbert space, for the seemingly paradoxical reason that most states are too entangled to be computationally useful [7].

The above picture is affected by symmetry. Namely, in certain symmetry protected phases of matter [16–19], every ground state has the same computational power [13, 23–31]. This phenomenon has been termed ‘computational phases of quantum matter’ [23, 24]. Some of these computational phases have universal computational power [28–31]. Yet, a classification of universal resource states has to date remained elusive.

Investigations of MBQC have traditionally adopted a local perspective. In this view, a central lemma is that quantum gates can be simulated by applying local measurements to an entangled state. Consequently, every circuit model computation—that is, a series of gates—can be converted into a sequence of local measurements on an appropriate resource state. From this vantage point, MBQC functions as a modular protocol for translating circuit model computations into measurements: gate by gate, measurement by measurement. This locally focused perspective is rightful and important; indeed, this is how the universality of MBQC as a computational model is typically proved. It does not, however, tell the whole story of MBQC.

The present paper lays out a complementary, global perspective. Readers familiar with MBQC will readily identify one aspect of it, which is tellingly non-local: the computational output is a specific combination of measurement outcomes, which were registered over the course of the computation. In this way, the computational power of MBQC relies on correlations between different measurement outcomes, which are extracted over many distinct and generically distant locales in the resource state. This fact is neither here nor there in a local

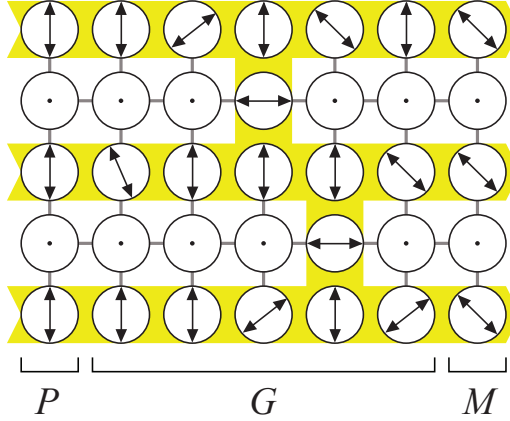


Figure 1: Graphical summary of MBQC with 2D cluster states. The circles represent the individual qubits of the cluster state, and the grey lines define the corresponding entanglement structure. The symbol \odot represents a measurement in the Z -basis, and the double-headed arrows are measurements in the eigenbasis of $\cos \alpha X + \sin \alpha Y$, for various angles α . The Z -measurements have the effect of removing the measured qubits from the cluster, leaving the remainder in a network-like structure. In a circuit model interpretation, the ‘horizontal’ direction represents circuit time (from left to right), and the ‘vertical’ direction labels the logical qubits in the simulated quantum register. The horizontal structures in yellow underlay represent sequences of one-qubit rotations, and the vertical bridges in yellow underlay mediate interaction between logical qubits.

view of MBQC, but it is an essential aspect of the computational scheme! Our quest for a global retelling of the MBQC story was initially motivated by this observation.

One topic in the undergraduate physics curriculum showcases a similar interplay between the local and the global: gauge theory. In the local perspective, defining a gauge theory starts with a vector potential $A_\mu(x)$, which is a local but unphysical quantity. It is unphysical because it is subject to gauge transformations, i.e. local symmetries of the theory. As the local symmetry acts independently at every location, it strips $A_\mu(x)$ off independent physical meaning because it can always locally reset it to an arbitrary different value. But this does not make $A_\mu(x)$ redundant. As famously explained by Aharonov and Bohm, the global object $\oint dx^\mu A_\mu(x)$ —a Wilson loop—measures an unambiguously defined, physical flux. Wilson loops are nonlocal, but they comprise the genuine degrees of freedom of a gauge theory. These facts show an uncanny resemblance to MBQC. Our task in this paper is to explain that this resemblance is not skin-deep or accidental. We argue that MBQC in all its aspects—global and local—is in fact naturally described by the language of gauge theory.

There is another reason why gauge theory could be suspected to play a role in MBQC. On one-dimensional cluster states, MBQC can be understood as a sequence of quantum half-teleportations [32]. However, as explained in Reference [33] (see also [34]), the effect of quantum teleportation is indistinguishable from the effect of a background gauge field on a charged particle traveling through space. While the argument in [33] assumed post-

selection on projective measurements, we of course know that any measurement outcome in an appropriate basis affords teleportation if the recipient applies a corrective gate on her end. If we now return to the discussion where teleportation and gauge theory are unified, the application of that corrective gate plays the role of a gauge transformation. This claim, which generalizes the analysis of [33] by eliminating the post-selection assumption, provides an important connection between MBQC and gauge theory.

To make the translation between MBQC and more familiar gauge theories transparent, we highlight the main entries of the proposed dictionary:

1. In MBQC, one progressively adjusts measurement bases depending on outcomes of prior measurements. These adjustments are gauge transformations; see Section 4.4.2.
2. The computational output of MBQC is a flux analogous to $\oint dx^\mu A_\mu(x)$; see Section 4.3.
3. Programming MBQC—the choice of quantum algorithm—amounts to choosing a basis, in which the flux is measured; see Section 5.4.

The gauge theory perspective is directly connected to symmetry-protected topological (SPT) order, which characterizes one class of states in the computational phase of quantum matter, including the one-dimensional cluster state. Although SPT order has long been known to play an important role in MBQC, we now understand that role on a more formal level: the symmetry, which protects the topological order, is our gauge symmetry.

A final point worth emphasizing is that the present paper is limited to MBQC on a one-dimensional cluster state. This setting allows MBQC to simulate arbitrary $SU(2)$ gates but not larger unitaries, and falls short of universality. The universal, two-dimensional case will be treated in a future publication.

For whom the paper is written, and why A target audience for this paper is quantum information theorists and condensed matter theorists, who are interested in unifying the various guises of MBQC under a common formalism. MBQC exemplifies many ideas that are of current relevance in high-energy and condensed matter physics, such as holographic duality [35–37] and bulk-boundary correspondence [24, 38, 39], the emergence of temporal order [21, 22], and topological order in 3D [40–43]—in the setting of quantum information processing. Recently, the subject of symmetry-protected topological order has contributed to the endeavor of exposing the fundamental structures of MBQC, and here we identify a further ingredient: gauge theory. We have kept the discussion of MBQC self-contained, so physicists outside the quantum information and condensed matter communities should find it easy to digest.

We use the one-dimensional cluster state as a main stage of presentation. This considerably simplifies the discussion while permitting to lay out the general tenet. It shall be noted, however, that universal measurement-based quantum computation requires cluster states in dimension two or higher.

Organization Section 2 is a pedagogical review of background material, including the one-dimensional cluster state and the MBQC protocol. Section 3 sets the stage for the formulation of the MBQC gauge theory by assigning group labels for the MBQC measurement basis using the MPS symmetries of the cluster state. In section 3.3, we formulate MBQC on a ring-like cluster state, which manifests most cleanly the gauge-theoretic character of MBQC. Section 4—the most important part of the paper—organizes the material in Sections 2 and 3 into concepts from gauge theory: a covariant derivative, reference sections, gauge transformations, and fluxes. Section 5 discusses the phenomenological implications of the MBQC gauge symmetry and shows how the gauge theoretical formulation sheds light on the relation between MBQC and the circuit model. We close the paper with a discussion of future directions.

2 Review of measurement-based quantum computation

Throughout this paper, we write the Pauli operators as $\sigma_x =: X$, $\sigma_y =: Y$, $\sigma_z =: Z$, and use a subscript j to indicate when the Pauli matrix acts on the j^{th} qubit. We let $|\pm\rangle$ be the eigenstates of X with eigenvalues ± 1 . We will often refer to these eigenstates using a binary variable s according to $|(-)^s\rangle$, that is $s = 0$ stands for $|+\rangle$ and $s = 1$ stands for $|-\rangle$. We will also need a notation for eigenstates of $O(\alpha) = (\cos \alpha)X + (\sin \alpha)Y$; they will be denoted with $|\pm_\alpha\rangle$. Measurements of $O(\alpha)$ will also be referenced using a binary variable s according to $|\pm_\alpha\rangle = |(-)^s_\alpha\rangle$.

2.1 The one-dimensional cluster state

The one-dimensional cluster state is a resource state for MBQC, which affords enough computational power to simulate $SU(2)$ gates. For reasons which will become clear in Section 5.4.1, we denote the cluster state as $|1\rangle$.

Teleportation and the cluster state The logical processing in MBQC may be understood as a sequence of teleportations. A resource state can be extracted by reordering commuting operations in a sequence of teleportation steps. The circuit for quantum telepor-

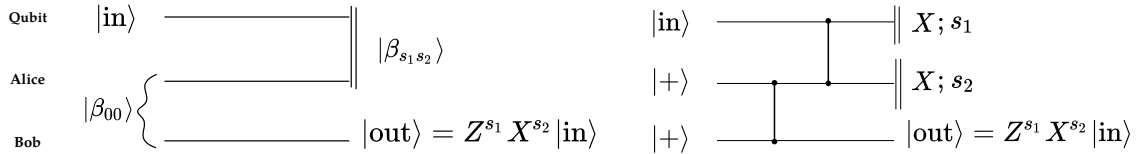


Figure 2: Circuit diagram for quantum teleportation.

tation is shown in the left panel of Figure 2. Alice and Bob share a prearranged resource state in the form of a Bell pair $|\beta_{00}\rangle := 2^{-1/2}(|11\rangle + |00\rangle)$. To teleport an initial qubit $|\text{in}\rangle$, Alice makes a measurement in the Bell basis, which comprises states $|\beta_{s_1 s_2}\rangle = X_1^{s_2} Z_1^{s_1} |\beta_{00}\rangle$ with $s_i = 0, 1$. (The subscripts in X_1 and Z_1 refer to the first qubit of the Bell pair.) Because

Alice does not control the random outcome of this measurement, the teleported qubit ends up rotated by a known but random byproduct operator

$$V_{s_2 s_1} = X^{s_2} Z^{s_1} \quad \text{where } s_i = 0, 1. \quad (2.1)$$

In this way, teleportation defines a randomly *fluctuating* circuit.

This randomness poses a challenge to our ability to perform the most basic computation: to simulate the identity gate on the teleported qubit. Luckily, Bob can undo the effect of the fluctuation because the measurement outcomes (s_2, s_1) are known to Alice, who passes them on to him by classical channels. Once Bob learns the measurement outcome, he can apply the inverse of the byproduct (2.1) and recover $|\text{in}\rangle$. What is equally important for the purposes of this paper, the measurement outcomes are related by a symmetry. The byproduct operators (2.1) form a projective representation of $\mathbb{Z}_2 \times \mathbb{Z}_2$, that is they respect the group operation

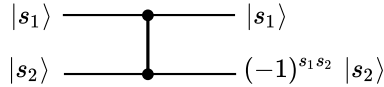
$$(s_2, s_1) + (s'_2, s'_1) = (s_2 + s'_2, s_1 + s'_1) \pmod{2} \quad (2.2)$$

up to a multiplicative phase. While the group operation (2.2) is not essential in a single instance of quantum teleportation, it makes for a key simplification when multiple teleportations are conducted in sequence. For example, after N sequential teleportations, Bob can apply a single corrective operator to invert

$$B = X^{\left(\sum_{j \text{ even}}^{2N} s_j\right)} Z^{\left(\sum_{j \text{ odd}}^{2N-1} s_j\right)} \quad (2.3)$$

and recover the initial state $|\text{in}\rangle$ up to a phase. We argue that this simplification, which is essential for MBQC, is best understood in the language of gauge theory. The $\mathbb{Z}_2 \times \mathbb{Z}_2$, which permutes the random measurement outcomes in each step, plays the role of a gauge group.

A resource state for a single instance of quantum teleportation is the Bell pair $|\beta_{00}\rangle$. A resource state for MBQC must, in a similar fashion, enable multiple teleportations in a sequence. Such a resource is constructed by putting together many copies of the circuit in Figure 2 as building blocks. Before the building blocks are assembled, it is useful to redraw them using the cPhase gate



$$\text{cPhase}(i, j) := \mathbb{I}_{i,j} - \frac{(\mathbb{I}_i - Z_i)(\mathbb{I}_j - Z_j)}{2} \quad (2.4)$$

as is done in the right panel of Figure 2. In equation (2.4), i and j label the two qubits on which cPhase acts. The redrawing reveals that Alice's measurement in the $|\beta_{s_1 s_2}\rangle$ basis is equivalent to measurements in the X -basis on the state shown in Figure 3.

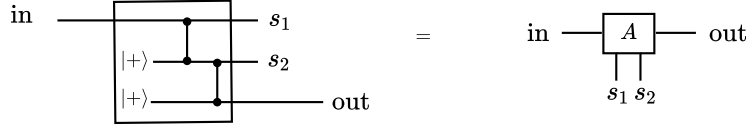


Figure 3: MPS tensor from the teleportation circuit.

To enable multiple teleportations to proceed in a sequence, we concatenate copies of Figure 3, identifying the $\langle \text{out} |$ leg of one copy with the $|\text{in}\rangle$ leg of the next copy. The state obtained this way is a matrix product state (MPS) and Figure 3 represents its MPS tensor. This MPS state—the one-dimensional cluster state $|1\rangle$ —is shown in Figure 4.

The cluster state as a matrix product state It is important to distinguish two Hilbert spaces involved in the MPS tensor. Alice’s measurement of the indices marked $s_2 s_1$ in Figure 3 effects quantum teleportation—a linear map from $|\text{in}\rangle$ to $|\text{out}\rangle$. As such, the MPS tensor is an (s_2, s_1) -dependent linear map $A_{s_2 s_1}$ with matrix elements $\langle \text{out} | A_{s_2 s_1} | \text{in} \rangle$. In discussions of MPS states, it is standard terminology to call the Hilbert space spanned by $|\text{in}\rangle$ and $|\text{out}\rangle$ the virtual space or correlation space, while the Hilbert space denoted by the subscript $s_2 s_1$ is referred to as the physical space. Virtual space is called virtual because, when the $\langle \text{out} |$ leg of one MPS tensor is joined with the $|\text{in}\rangle$ leg of the next (when two teleportations are conducted in a sequence), we lose direct physical access to that degree of freedom. The physical space is called physical because it is always physically accessible; it is the space where Alice makes her measurements.

Our discussion should make clear that the MPS tensor $A_{s_2 s_1}$ in the X -basis equals the byproduct $V_{s_2 s_1}$ from equation (2.1). The cluster state on a ring of $2N$ qubits is obtained by contracting N copies of this MPS tensor:

$$|1\rangle = \mathcal{N} \sum_{(s_{2j}, s_{2j-1}) \in \mathbb{Z}_2 \times \mathbb{Z}_2} \text{Tr}(A_{s_{2N}, s_{2N-1}} \cdots A_{s_4, s_3} A_{s_2, s_1}) |s_{2N}, s_{2N-1}\rangle \cdots |s_4, s_3\rangle |s_2, s_1\rangle \quad (2.5)$$

Each $|s_{2j}, s_{2j-1}\rangle$ is a two-qubit state taken from $\{|++\rangle, |+-\rangle, |-+\rangle, |--\rangle\}$, labeled with an element $(s_{2j}, s_{2j-1}) \in \mathbb{Z}_2 \times \mathbb{Z}_2$. We use the generic notation $A_{(s_{2j}, s_{2j-1})}$ for the MPS tensor rather than $V_{(s_{2j}, s_{2j-1})}$ since we will later be interested in evaluating the same tensor in a different basis. Here and in similar formulas below the factor \mathcal{N} ensures a proper normalization of the state.

Throughout this paper, the notation ‘ $|1\rangle$ ’ shall stand for the 1D cluster state, not for a computational basis state. The reason for this notation will become clear later. In short, the cluster state is identified as an eigenstate of a flux observable with eigenvalue 1.

For a chain-like cluster state, the traces in the amplitudes are replaced by analogous expressions, which depend on a choice of boundary conditions at endpoints:

$$\text{Tr}(A_{s_{2N}, s_{2N-1}} \cdots A_{s_4, s_3} A_{s_2, s_1}) \longrightarrow \langle \text{out} | A_{s_{2N}, s_{2N-1}} \cdots A_{s_4, s_3} A_{s_2, s_1} | \text{in} \rangle \quad (2.6)$$

A glimpse of a global structure. Equation (2.5) offers a first sighting of the kind of global structure, which we seek to identify. This comes in the form of a global selection rule, which determines which combinations of physical spins do / do not overlap with the ring-like cluster state.

The amplitudes in (2.5) involve products of projective representation matrices of $\mathbb{Z}_2 \times \mathbb{Z}_2$. We can use the group multiplication $A_{(s_{2j+2}, s_{2j+1})} A_{(s_{2j}, s_{2j-1})} \propto A_{(s_{2j+2}, s_{2j+1}) + (s_{2j}, s_{2j-1})}$ to simplify them:

$$|1\rangle = \mathcal{N} \sum_{(s_{2j}, s_{2j-1}) \in \mathbb{Z}_2 \times \mathbb{Z}_2} (\text{phase}) \times (\text{Tr} A_{(s_{2N}, s_{2N-1}) + \dots + (s_4, s_3) + (s_2, s_1)} |s_{2N}, s_{2N-1}\rangle \dots |s_4, s_3\rangle |s_2, s_1\rangle) \quad (2.7)$$

Since every $A_{(\cdot)}$ except A_{++} is traceless, the wavefunction vanishes unless

$$(s_{2N}, s_{2N-1}) \dots (s_4, s_3) + (s_2, s_1) = (0, 0) \in \mathbb{Z}_2 \times \mathbb{Z}_2 \quad (2.8)$$

Component-wise, we thus have

$$a \equiv s_1 + s_3 + \dots + s_{2N-1} = 0 \quad \text{and} \quad b \equiv s_2 + s_4 + \dots + s_{2N} = 0 \pmod{2} \quad (2.9)$$

We will recast the selection rule (2.8-2.9) as a holonomy (a, b) of a $\mathbb{Z}_2 \times \mathbb{Z}_2$ gauge field. In this view, the cluster state on a ring represents a gauge theory state with trivial $\mathbb{Z}_2 \times \mathbb{Z}_2$ flux. Equivalently, the Wilson line around the cluster evaluates to $++$, which is the identity element of the group. This is a first reason why we denote the cluster state as $|1\rangle$, though a more complete explanation will be given in Section 5.4.1.

Readers familiar with MBQC will recognize the meaning of this discussion. When we measure $|1\rangle$ in the $|\pm\rangle$ basis, we effectively simulate the identity gate. This simulation happens to have a fully deterministic outcome—reflecting the fact that $|1\rangle$ is a state of definite $++$ (identity) flux.

The cluster state is short ranged entangled Figure 3 shows that the MPS tensor can be constructed by acting with two-qubit entangling gates (2.4) on a product state. Naturally, the same can be said about the full MPS state. The left panel of Figure 4 shows (a segment of) the cluster state, constructed by repeated applications of the cPhase gate on a product state. As an equation, we have:

$$|1\rangle := \prod_{i=1}^{2N-1 \text{ or } 2N} \text{cPhase}(i, i+1) \left(\bigotimes_{j=1}^{2N} |+\rangle_j \right) \quad (2.10)$$

The $(2N)^{\text{th}}$ gate $\text{cPhase}(2N, 2N+1) \equiv \text{cPhase}(2N, 1)$ is only applied on a ring, where we define $2N+1 \equiv 1$. Note that all cPhases commute because they are simultaneously diagonal in the Z -eigenbasis.

As seen in Figure 4, the preparation of the cluster from the product state $\bigotimes_j |+\rangle_j$ can be

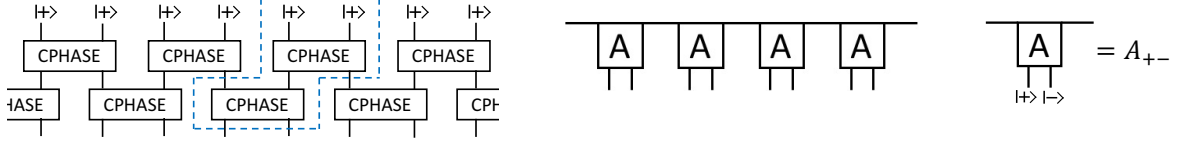


Figure 4: The cluster state, as given by equation (2.10) (left) and in its MPS form (middle). The highlighted part of the left panel is one matrix of the MPS description (right); it covers one ‘block.’

achieved in two time steps: the application of the $\text{cPhases}(i, i+1)$ with i odd, and with i even. Because the cluster state can be prepared by a circuit of finite depth (two), it is short range-entangled. This demonstrates that using the cluster state for quantum computation does not introduce hidden costs associated with the preparation of the initial state.

The cluster state as a stabilizer state. Equation (2.10) reveals that $|1\rangle$ is a stabilizer state [44, 45]. Because every X_j stabilizes $\otimes_j |+\rangle_j$, conjugating X_j by the cPhases in (2.10) gives a stabilizing operator for $|1\rangle$. Using the identity $\text{cPhase}(i, j)X_i\text{cPhase}(i, j) = X_iZ_j$, we find the following stabilizers:

$$K_j |1\rangle = |1\rangle \quad \text{with} \quad K_j := Z_{j+1}X_jZ_{j-1} \quad (2.11)$$

On a ring, these equations completely determine $|1\rangle$. On a chain indexed by $1 \leq j \leq 2N$, equation (2.11) makes no sense for $j = 1$ or $2N$. In that context, in addition to (2.11), the chain-like cluster state is also stabilized by two special operators Z_2X_1 and $X_{2N}Z_{2N-1}$. The K_j with $2 \leq j \leq 2N-1$, along with the two special stabilizers at endpoints, completely determine the cluster state on a chain. For future use, we remind the reader that each K_j squares to the identity.

The stabilizer conditions (2.11) translate the entanglement structure of the cluster state into a set of algebraic constraints, which can be solved explicitly by summing over orbits of the stabilizers:

$$|1\rangle \propto \prod_i \left(\frac{1 + K_i}{2} \right) \left(\bigotimes_{j=1}^{2N} |+\rangle_j \right) \quad (2.12)$$

The structure of these constraints as well as their solution mirrors the structure of gauge constraints, which is why we will be able to embed the cluster state into a gauge theory. The stabilizer conditions play an important role in mitigating the randomness of measurement outcomes in MBQC. Much of our paper is devoted to understanding this feature of MBQC in terms of a gauge symmetry. For a preview of this interpretation, observe that for any operator O , conjugation by a stabilizer does not affect expectation values taken in $|1\rangle$:

$$\langle 1 | K_j O K_j | 1 \rangle = \langle 1 | O | 1 \rangle \quad (2.13)$$

This means that, so long as we work with the cluster state $|1\rangle$, it is redundant and unnecessary to distinguish O from $K_j O K_j$. For a technician operating on $|1\rangle$, the difference between O and $K_j O K_j$ is a redundancy of description—a redundancy, which markedly resembles a gauge symmetry.

Because the stabilizers K_j commute with one another, the full stabilizer group of the cluster state is isomorphic to \mathbb{Z}_2^{2N} . In fixing a ‘stabilizer gauge,’ one independent binary choice—to apply or not to apply K_j (as in (2.12))—is available at every qubit j . The independence of these choices agrees with the understanding of gauge symmetry as a *local* symmetry, one \mathbb{Z}_2 per qubit. In fact, the K_j s which act on even and odd sites can be meaningfully distinguished from one another. We will see that this implies the cluster state supports a $\mathbb{Z}_2 \times \mathbb{Z}_2$ gauge symmetry, and that the gauge character of this symmetry is an essential component of MBQC.

2.2 MBQC

Here we review MBQC on a chain, following the treatment of [20] in the MPS formalism. In Section 2.2.1 we introduce the idea of a logical quantum register propagating in the MPS virtual (or correlation) space, first for the special instance where all measurements are performed in the local X -basis. In Section 2.2.2 we introduce more general local measurement bases, leading to more MBQC-simulated quantum gates. In Section 2.2.3 we describe how to extract the computational output from the measurement record.

2.2.1 Basic idea

To begin, we write down the cluster state on a chain as defined by equations (2.5) and (2.6):

$$|1\rangle = \mathcal{N} \sum_{s_j \in \mathbb{Z}_2} \left(\langle \text{out} | A_{s_{2N}, s_{2N-1}} \cdots A_{s_4, s_3} A_{s_2, s_1} | \text{in} \rangle \right) |s_{2N}, s_{2N-1}\rangle \cdots |s_4, s_3\rangle |s_2, s_1\rangle.$$

At present, we consider the above expansion in the local X -basis only. This restriction will subsequently be lifted. One way to interpret this formula is as a sum over trajectories, which an input state $|\text{in}\rangle$ follows under successive applications of operators $A_{s_{2j}, s_{2j-1}}$. In a laboratory, an experimenter can (partly) control these trajectories by projecting the cluster state onto chosen states of successive qubits. To wit, measuring the first two qubits in the $\langle s_2, s_1 |$ basis applies the gate $A_{s_2, s_1} = V_{s_2, s_1}$:

$$\langle s_2, s_1 | 1 \rangle = \mathcal{N}' \sum_{s_j \in \mathbb{Z}_2} \left(\langle \text{out} | A_{s_{2N}, s_{2N-1}} \cdots A_{s_4, s_3} V_{s_2, s_1} | \text{in} \rangle \right) |s_{2N}, s_{2N-1}\rangle \cdots |s_4, s_3\rangle \quad (2.14)$$

Note that the matrix V_{s_2, s_1} , which is left inside the amplitude after the $\langle s_2, s_1 |$ projection, is not an MPS tensor anymore because its physical indices are no longer summed over. This is why we denote it as V_{s_2, s_1} and not A_{s_2, s_1} ; see the comment above equation (2.5). A sequence

of projections determines a longer trajectory:

$$\dots \longleftarrow V_{s_6, s_5} V_{s_4, s_3} V_{s_2, s_1} |\text{in}\rangle \longleftarrow V_{s_4, s_3} V_{s_2, s_1} |\text{in}\rangle \longleftarrow V_{s_2, s_1} |\text{in}\rangle \longleftarrow |\text{in}\rangle \quad (2.15)$$

MBQC uses such trajectories to realize quantum computation. Indeed, (2.15) can be viewed as a simulation of a computation in the circuit model, in which the applied gates are of the form (2.1). The lab technician, who projects $|1\rangle$ onto chosen single qubit states, is a quantum computer programmer. In the final step of this quantum computation, the last state on the trajectory

$$V_{s_{2N}, s_{2N-1}} \dots V_{s_4, s_3} V_{s_2, s_1} |\text{in}\rangle = (\text{phase}) \times V_{(s_{2N}, s_{2N-1}) + \dots + (s_2, s_1)} |\text{in}\rangle \quad (2.16)$$

is measured in some basis $\langle \text{out} |$ to produce one classical bit of computational output.

The above description leaves out two important aspects of MBQC. The first one concerns the set of quantum gates, which MBQC can simulate. Thus far, we have only drawn gates from (2.1), but for realizing general $SU(2)$ transformations a larger gate set is necessary. This will require a generalization of the quantum teleportation protocol, in which the measurement basis is modified. The second wanting point, which is conceptually more important, is about control over measurement outcomes. The preceding discussion pretended that the technician could project $|1\rangle$ onto chosen qubit states at will, but of course every quantum measurement is probabilistic. When the technician does not obtain her planned outcome, the virtual qubit in (2.15) takes an unplanned turn. For a complete definition of MBQC, we must give a protocol to address both of those outstanding points. We do so presently.

2.2.2 Measurement basis and temporal order

In order to simulate an arbitrary $SU(2)$ gate, MBQC generalizes the teleportation protocol by measuring the cluster state in a rotated basis on the XY plane. To prevent the randomness of measurement outcomes from contaminating the quantum computation, future measurement angles must be adapted based on past outcomes. These two features can be achieved by measurements in a temporally ordered basis, given by

$$O((-)^{q_i} \alpha_i) := \cos(\alpha_i) X + \sin((-)^{q_i} \alpha_i) Y, \quad (2.17)$$

where

$$q_i = s_{i-1} + s_{i-3} + \dots + (s_2 \text{ or } s_1). \quad (2.18)$$

Here s_i denotes the measurement outcome for measuring along $(-)^{q_i} \alpha_i$. The parameters q_i tell the experimenter measuring the i^{th} qubit to adapt the sign of α_i based on results of previous measurements. Eq. (2.18) is one of the two *classical side processing relations* of MBQC. It governs the adaptation of measurement bases to account for the randomness of earlier measurement outcomes.

To understand the adapted basis (2.18) in the simplest setting, consider measurements on

a single *block* of two sites. (We will refer to consecutive pairs of spins as ‘blocks’ throughout the paper; cf. Figure 4.) Let us denote the projection of the MPS tensor onto $O(\alpha_i)$ -eigenstates with $A_{s_2 s_1}(\alpha_2, \alpha_1)$. Equation (2.18) instructs us to flip the sign of α_2 based on the result of measuring the first spin along α_1 because $q_2 = s_1$. Doing so results in the following operators acting on the virtual space:

$$\begin{aligned} A_{++}(\alpha_2, \alpha_1) &= V_{++} U \\ A_{-+}(\alpha_2, \alpha_1) &= V_{-+} U \\ A_{+-}(-\alpha_2, \alpha_1) &= V_{+-} U \\ A_{--}(-\alpha_2, \alpha_1) &= V_{--} U \end{aligned} \quad (2.19)$$

where

$$U = \exp\left(-i\frac{\alpha_2}{2}X\right) \exp\left(-i\frac{\alpha_1}{2}Z\right) = A_{++}(\alpha_2, \alpha_1) \quad (2.20)$$

and $V_{s_2 s_1}$ was defined in (2.1). These equations generalize teleportation, in the sense that the ‘teleported’ input state arrives rotated by a unitary transformation U , up to a random byproduct operator $V_{s_2 s_1}$. Ordinary teleportation corresponds to $U = 1$ and is recovered when $\alpha_i = 0$.

Now consider a cluster chain with N blocks, that is $2N$ spins. We find in eq. (2.19) that for all four combinations of measurement outcomes, the unitary U is the same, and the evolution of the virtual system differs only by the random byproduct operator. The byproduct operators V are all of Pauli type.

These random byproduct operators, one produced by each measurement, need to be removed from the computation. This is achieved by propagating them forward in time, through the not yet implemented part of the computation, and past the logical readout measurements. What happens after logical readout doesn’t affect the computational output.

Inspecting equation (2.20), we find:

$$A_{++}(\alpha_2, \alpha_1)X = X A_{++}(\alpha_2, -\alpha_1) \quad \text{and} \quad A_{++}(\alpha_2, \alpha_1)Z = Z A_{++}(-\alpha_2, \alpha_1). \quad (2.21)$$

The forward-propagation of the byproduct operators flips angles of rotations on virtual space, and those flips have to be compensated by flips of the measurement angle, cf. Eq. (2.17). The binary observables q_i account for this. With eqs. (2.1) and (2.20) we verify that the sign flip of the measurement angle on an even site depends on the parity of all measurement outcomes on earlier odd sites, and the sign flip of the measurement angle on an even site on the parity of the measurement outcomes of the earlier odd sites. This is the content of the classical processing relation (2.18).

Denoting the MPS tensor in the adapted basis by

$$A_{s_{i+1}, s_i; q_{i+1}, q_i} := A_{s_{i+1}, s_1}((-1)^{q_{i+1}}\alpha_{2N}, (-1)^{q_i}\alpha_{2N-1}), \quad (2.22)$$

the result of the byproduct propagation can be summarized by

$$A_{s_{2N}, s_{2N-1}; q_{2N}, q_{2N-1}} \cdots A_{s_2, s_1; q_2, q_1} = B U_{\text{total}}, \quad (2.23)$$

where

$$B = V_{s_{2N}, V_{2N-1}} \dots V_{s_4, s_3} V_{s_2, s_1} = (\text{phase}) \times V_{(s_{2N}, s_{2N-1} + \dots + (s_2, s_1))}, \quad (2.24)$$

$$U_{\text{total}} = A_{++}(\alpha_{2N}, \alpha_{2N-1}) \dots A_{++}(\alpha_4, \alpha_3) A_{++}(\alpha_2, \alpha_1). \quad (2.25)$$

We now recognize that equation (2.17) is designed to render (2.25)—so that the adapted measurements always simulate the same unitary transformation U_{total} .

Equation (2.23) is the most important result of the MBQC protocol. It shows that when the cluster state is measured in the adapted basis, the ‘teleported’ qubit arrives rotated by U_{total} , up to a known byproduct operator B for which the recipient must correct. In Section 4.2 we explain that B functions as a $\mathbb{Z}_2 \times \mathbb{Z}_2$ Wilson line.

Simulating a general unitary Finally, observe that a general $SU(2)$ gate can be generated by measuring four qubits:

$$A_{++}(0, \alpha_3) A_{++}(\alpha_2, \alpha_1) = \exp\left(-i \frac{\alpha_3}{2} Z\right) \exp\left(-i \frac{\alpha_2}{2} X\right) \exp\left(-i \frac{\alpha_1}{2} Z\right) \quad (2.26)$$

This expression parametrizes the $SU(2)$ manifold with Euler angles $\alpha_{1,2,3}$. We conclude that measurements of $|1\rangle$ in the $O(\alpha)$ eigenbasis can simulate every $SU(2)$ gate on virtual space so long as the effect of byproduct operators—an imprint of the randomness of measurement outcomes—can be properly remedied.

2.2.3 Computational output for MBQC on a chain

After qubits 1 through $2N$ of a chain-like cluster state have been measured in the adapted basis, the experimenter gets a probability distribution, which depends on the boundary condition $\langle \text{out} |$ at the other end. Instead of a preordained boundary condition, we will follow the logic of equation (3.16) and treat the choice of $\langle \text{out} |$ as one final projective measurement, applied to the $(2N + 1)^{\text{st}}$ qubit in the state:

$$(\text{phase}) \times B U | \text{in} \rangle \quad (2.27)$$

The B and U are given in (2.24-2.25) and we drop the subscript ‘total’ from U .

In the circuit model of quantum computing, the application of a gate U to an initial state $|\text{in}\rangle$ is followed by a measurement of $U|\text{in}\rangle$ in some orthogonal basis, for example $\langle \pm |$. The computational output is sampled from the resulting probability distribution $p_{\pm} = |\langle \pm | U |\text{in}\rangle|^2$.

In MBQC, we mirror that last step by measuring state (2.27) in an orthogonal basis $\langle \text{out}_{\pm} |$, with $\langle \pm |$ being a canonical choice. The hitherto unfixed choice of boundary condition $\langle \text{out} |$ at the end of the chain represents the choice of basis for the final measurement, whose outcome serves as the computational output.

In equation (2.27), the randomness of prior measurement outcomes remains visible in the byproduct operator B . For a computational output that is free of randomness, we again adjust the measurement basis and project state (2.27) onto $\langle \text{out}_{\pm} | B$ instead of $\langle \text{out}_{\pm} |$. This

works because $B^2 = \pm 1$ implies:

$$\langle \text{out}_\pm | B (\text{phase}) \times B U | \text{in} \rangle = (\text{phase}) \times \langle \text{out}_\pm | U | \text{in} \rangle \quad (2.28)$$

When the final measurement is done in the X -eigenbasis $\langle \text{out}_\pm | = \langle \pm |$, the adjustment $\langle \text{out}_\pm | \rightarrow \langle \text{out}_\pm | B$ is particularly simple. Let us write the byproduct B in terms of the ‘holonomy’ variables (a, b) from (2.9):

$$B = X^b Z^{\tilde{a}} \quad \text{with} \quad \tilde{a} = \sum_{j \text{ odd}}^{2N-1} s_j \quad \text{and} \quad b = \sum_{j \text{ even}}^{2N} s_j \quad (2.29)$$

We ignore the possible phase because it will drop out of the reported probability distribution $p_\pm = |\langle \text{out}_\pm | U | \text{in} \rangle|^2$. Letting $\langle \text{out}_\pm | := \langle s_{2N+1} |$, we see that the byproduct transforms the final projection basis as:

$$\langle s_{2N+1} | B = \langle s_{2N+1} + \tilde{a} | := \langle a | \quad (2.30)$$

Accordingly, we define the computational output as:

$$a := s_{2N+1} + \tilde{a} = s_1 + s_3 + \dots + s_{2N-1} + s_{2N+1} \quad (2.31)$$

Eq. (2.31) is the second classical processing relation of MBQC. Together with eq. (2.18), which governs the adaptation of measurement bases, it is responsible for compensating the randomness inherent in the quantum measurements driving MBQC.

The probability $p(a)$ of observing the output $a = 0, 1$ is exactly equal to the probability $p(a) = |\langle a | U | \text{in} \rangle|^2$ for the corresponding quantum circuit realizing the unitary U and finding a upon readout.

Equation (2.31) puts all $2N + 1$ measurements on equal footing. Here, again, a global structure that underlies MBQC becomes evident. We have advertised in the Introduction, and we argue in Section 4.2, that the MBQC computational output is (one component of) a Wilson line of a $\mathbb{Z}_2 \times \mathbb{Z}_2$ gauge field.

3 Preparations for the MBQC gauge theory

To set the stage the presentation of the MBQC gauge theory in Section 4, we introduce two additional ingredients in this section: a group valued label for the measurement outcomes with respect to the adapted basis (2.17), and an algorithm for performing MBQC on a ring.

3.1 $\mathbb{Z}_2 \times \mathbb{Z}_2$ action and MPS tensor symmetries

We begin by reviewing the relevant representations of $\mathbb{Z}_2 \times \mathbb{Z}_2$ on the physical Hilbert space and the transformation laws of the MPS tensor under these symmetries [18, 25]. There are two projective representations of $\mathbb{Z}_2 \times \mathbb{Z}_2$, which we refer to as $l(g)$ and $r(g)$. Using the

multiplicative mod 2 notation $g = (\pm, \pm) \in \mathbb{Z}_2 \times \mathbb{Z}_2$, their action on each block of physical qubits are:

$$l(++) = 1 \otimes 1, \quad l(+-) = X_2 \otimes Z_1, \quad l(-+) = Z_2 \otimes 1, \quad l(--)= Z_2 X_2 \otimes Z_1 \quad (3.1)$$

$$r(++) = 1 \otimes 1, \quad r(+-) = 1 \otimes Z_1, \quad r(-+) = Z_2 \otimes X_1, \quad r(--)= Z_2 \otimes X_1 Z_1 \quad (3.2)$$

We refer to these as the left and right action of $\mathbb{Z}_2 \times \mathbb{Z}_2$. The product

$$u(g) := l(g)r(g) \quad (3.3)$$

generates a linear representation $\mathbb{Z}_2 \times \mathbb{Z}_2$ which acts by X on even and odd sites:

$$u(++) = 1 \otimes 1, \quad u(+-) = X_2 \otimes 1, \quad u(-+) = 1 \otimes X_1, \quad u(--)= X_2 \otimes X_1 \quad (3.4)$$

The MPS tensor satisfies a set of equivariant transformation laws under (3.1-3.4). These are illustrated graphically in Figure 5. They relates the action of $\mathbb{Z}_2 \times \mathbb{Z}_2$ on the physical and virtual degrees of freedom, giving the experimentalist indirect access to correlation space via manipulations on physical qubits.

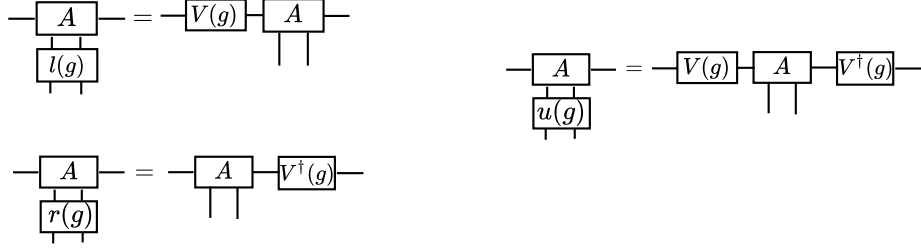


Figure 5: The left panels show the equivariant transformation law of the cluster MPS tensor under the left $l(g)$ and right $r(g)$ action of $\mathbb{Z}_2 \times \mathbb{Z}_2$. Composing these gives the transformation under $u(g) = l(g)r(g)$. More generally, analogous group actions and transformation laws apply to the fixed point MPS of any SPT phase protected by an onsite G symmetry [18, 49].

3.2 Group labels for measurement outcomes

We can use the left action $l(\mathbb{Z}_2 \times \mathbb{Z}_2)$ to assign a group label to the measurement outcomes in each block. For simplicity let us begin with a chain containing only a single block. $l(g)$ acts on the $O(\alpha_i)$ eigenstates according to the commutation relations:

$$\begin{aligned} X_i O(\alpha_i) &= O(-\alpha_i) X_i \\ Z_i O(\alpha_i) &= -O(\alpha_i) Z_i \end{aligned} \quad (3.5)$$

In effect, Z_i flips the measurement outcomes s_i . X_i , on the other hand, flips the sign of α_i but leaves s_i invariant. Because equation (3.1) features X_2 only in the combination $X_2 \otimes Z_1$, we

see that α_2 gets flipped only when $s_1 = 1$. Equation (2.17) encodes this fact in the classical processing relation $q_2 = s_1$.

Under the action of this symmetry, the locally adapted basis

$$|+\alpha_2\rangle \otimes |+\alpha_1\rangle \quad \text{and} \quad |+(-\alpha_2)\rangle \otimes |-\alpha_1\rangle \quad \text{and} \quad |-\alpha_2\rangle \otimes |+\alpha_1\rangle \quad \text{and} \quad |-(-\alpha_2)\rangle \otimes |-\alpha_1\rangle \quad (3.6)$$

forms an orbit under $\mathbb{Z}_2 \times \mathbb{Z}_2$. Therefore, we can label the basis vectors by group elements using $|+\alpha_2\rangle \otimes |+\alpha_1\rangle$ as a reference:

$$|g\rangle = l(g) |+\alpha_2\rangle \otimes |+\alpha_1\rangle, \quad \text{where } g \in \mathbb{Z}_2 \times \mathbb{Z}_2 \quad (3.7)$$

Thus, the measurement outcomes can be identified with elements of $\mathbb{Z}_2 \times \mathbb{Z}_2$. We use the same group label to denote the MPS tensor components (2.20) with respect to the adapted basis (3.7):

$$A_g := A_g((-)^{s_1} \alpha_2, \alpha_1), \quad (3.8)$$

where we will occasionally drop the argument of A_g when there is no risk of confusion.

When we measure the MPS tensor in the state $|g\rangle$, the equivariant transformation law under $l(g)$ (Figure 5) implies:

$$A_g = V_g U = V_g A_{++}(\alpha_2, \alpha_1) \quad (3.9)$$

This equation, presented graphically in Figure 6, succinctly summarizes (2.19) and explains its origin via the MPS symmetries. In Section 4, we interpret this equation as a discrete analogue of the covariant derivative in continuum gauge theory.

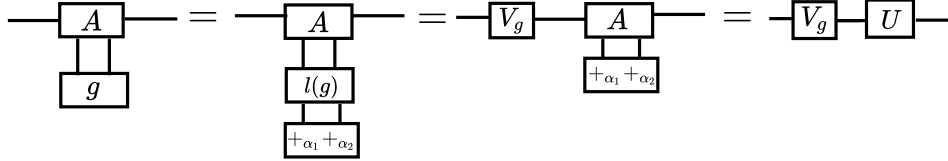


Figure 6: The MPS symmetry transformation under $l(g)$ can be applied to decompose each measured MPS tensor into an intended unitary U and a byproduct V_g .

3.2.1 Incorporating temporal order

Adaptation by symmetry The left action $l(g)$ which defines the states $|g\rangle$ in equation (3.7) accounts for the adaptation of measurement basis within a block, but does not account for the adaptation between different blocks. To incorporate these global adaptations, we have to change the reference state in (3.7) to depend on the previous outcomes. This modification can be achieved using the group action $u(g)$ [25]. To explain this, let us first reformulate the

basis adaptation between different blocks in terms of symmetry operations. This is illustrated in Figure 7. This first equality shows that the effect of obtaining an unwanted outcome

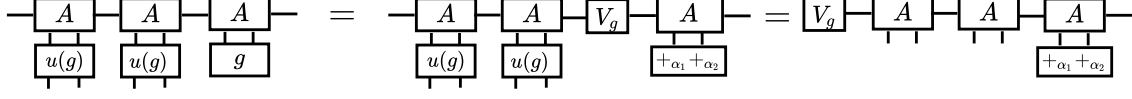


Figure 7: Adaptation of measurement basis can be implemented by applying $u(g)$.

g at the first block is to produce a byproduct operator in the virtual Hilbert space, which cannot be accessed directly. However, equipped with the symmetry operation $u(g)$, our MBQC programmer can cancel out any unwanted byproduct operator V_g in the interior of the chain by applying $u(g)$ to all yet-to-be-measured qubits. This sends the byproduct V_{g_i} to the end of the chain, where it joins other V_g 's in forming the byproduct B in equation (2.24). The effect of $u(g)$ on unmeasured qubits is captured by equations (3.5). As $u(g)$ contains only X operators, future measurement outcomes are undisturbed but even/odd measurement angles are flipped. Iterating this procedure for all interior V_{g_i} 's reproduces equation (2.23).

Group labels for the globally adapted basis By iterating the adaptation procedure in Figure 7, we find that the adaptation between different blocks is implemented by the cumulative action of $u(g)$ on the j^{th} block:

$$u(g_{\prec j}) = X^{s_{2j-3}+\dots+s_3+s_1} \otimes X^{s_{2j-2}+\dots+s_4+s_2} \\ g_{\prec j} := g_{j-1} \dots g_2 g_1 \quad (3.10)$$

Thus we can incorporate the global adaptation into the definition of $|g\rangle$ in by changing the reference basis to:

$$u(g_{\prec j}) |+\alpha_{2j}\rangle \otimes |+\alpha_{2j-1}\rangle = |+_{((-)^{q_{2j}-s_{2j-1}}\alpha_{2j})}\rangle \otimes |+_{((-)^{q_{2j-1}}\alpha_{2j-1})}\rangle \quad (3.11)$$

Relative to this reference state, the measurement basis at the j^{th} block¹ is:

$$|g_j\rangle = l(g_j) u(g_{\prec j}) |+\alpha_{2j}\rangle \otimes |+\alpha_{2j-1}\rangle \quad (3.13)$$

Using this notation, the cluster state in the globally adapted basis is simply given by:

$$|1\rangle = \mathcal{N} \sum_{g \in \mathbb{Z}_2 \times \mathbb{Z}_2} \left(\langle \text{out} | A_{g_N} \dots A_{g_2} A_{g_1} | \text{in} \rangle \right) |g_N, \dots, g_2, g_1\rangle \quad (3.14)$$

¹Explicitly, we can write (3.13) as

$$|g_j\rangle = l(g_j) |+_{((-)^{q_{2j}-s_{2j-1}}\alpha_{2j})}\rangle \otimes |+_{((-)^{q_{2j-1}}\alpha_{2j-1})}\rangle, \quad \text{where } g \in \mathbb{Z}_2 \times \mathbb{Z}_2 \quad (3.12)$$

Note how the adaptive parameter in front of α_{2j} excludes s_{2j-1} , so that the action of $X_{2j}Z_{2j-1}$ in $l(g)$ reproduces equation (2.17).

Here A_g denotes the MPS tensor measured in the globally adapted basis (3.13). To unpack this notation a bit, note that using the transformation laws in Figure 5, we can write:

$$A_{g_j} = V_{g_{\prec i}} (V_{g_j} U_{f_j}) V_{g_{\prec i}}^\dagger \quad (3.15)$$

Adaptation using stabilizers Consider a single step of the ‘adaptation by symmetry’ procedure shown in Figure 7. To cancel out the byproduct V_{g_i} at the end of the chain, we should apply $V_{g_i}^\dagger$ to the uncontracted virtual leg of the last MPS tensor. It is now useful to view this leg as a final, $(2N+1)^{\text{st}}$ qubit of a cluster chain of length $2N+1$. After doing so, the total transformation that corrects the measurement outcome g_i is:

$$\mathcal{K}_i(g_i) = \overbrace{V_{g_i}^\dagger}^{(2N+1)^{\text{st}} \text{ qubit}} \left(\prod_{j=i+1}^N u_j(g_i) \right) l_i(g_i) \quad (3.16)$$

Notice that this is a product of stabilizers. In particular, for the nontrivial generators $g_i = +-$ and $g_i = -+$ we have:

$$\begin{aligned} \mathcal{K}_i(+-) &= Z_{2N+1} (X_{2N} \cdots X_{2i+2} X_{2i}) Z_{2i-1} \\ \mathcal{K}_i(-+) &= X_{2N+1} (X_{2N-1} \cdots X_{2i+1}) Z_{2i} \end{aligned} \quad (3.17)$$

$\mathcal{K}_i(+-)$ is a telescoping product of $K_j = Z_{j+1} X_j Z_{j-1}$ while $\mathcal{K}_i(-+)$ combines K_j ’s with the special stabilizer $X_{2N+1} Z_{2N}$, which acts at the end of the chain.

Equivalent measurement records A stabilizer transformation manifestly leaves $|1\rangle$ invariant, but conjugates the operators $O(\alpha_i)$ as in equation (2.13). This in turn implies a nontrivial transformation of the classical processing data (q_i, s_i) :

$$\begin{aligned} K_j : s_{j-1} &\rightarrow s_{j-1} + 1 \\ s_{j+1} &\rightarrow s_{j+1} + 1 \\ q_j &\rightarrow q_j + 1 \end{aligned} \quad (3.18)$$

Finally, we observe that each stabilizer K_j can be expressed entirely in terms of projective representations of $\mathbb{Z}_2 \times \mathbb{Z}_2$. Recalling that the j^{th} block in the MPS description contains the $(2j-1)^{\text{st}}$ and the $(2j)^{\text{th}}$ qubit, we see that the stabilizers can be expressed as:

$$\begin{aligned} K_{2j} &= r_{j+1}(+-) l_j(+-) \\ K_{2j-1} &= r_j(-+) l_{j-1}(-+) \end{aligned} \quad (3.19)$$

3.3 MBQC on a ring

In a conventional treatment, MBQC stops at equation (2.31), having extracted from a simulation of a general single-qubit gate U one classical bit of computational output. Yet common

lore (technically known as the superdense coding protocol) implies that a single qubit ought to be equivalent to two bits of classical data. Working with a chain-like cluster state, we could try to recover another classical bit of data by varying the initial boundary condition $|\text{in}\rangle \rightarrow |\text{in}_\pm\rangle$, just like we did with the final boundary condition $\langle\text{out}_\pm|$. Doing so would probe the other \mathbb{Z}_2 component of the advertised $\mathbb{Z}_2 \times \mathbb{Z}_2$ Wilson line.

In fact, setting this up on a chain-like cluster state is an awkward exercise. The same benefit is achieved far more simply by placing the cluster state on a ring. The extra simplicity afforded by the ring topology mirrors facts from gauge theory. A closed integral of a gauge field such as $\oint dx^\mu A_\mu(x)$, called a Wilson loop, is automatically gauge invariant. Its line analogue, $\int_i^f dx^\mu A_\mu(x)$, called a Wilson line, is tainted by a gauge dependence at endpoints. For a gauge-invariant object on a line segment, a Wilson line must be combined with a charge at each end. In our discussion, the role of these charges is played by the variable boundary conditions $\langle\text{out}_\pm|$ and $|\text{in}_\pm\rangle$. Indeed, what achieves gauge-independence in equation (2.28) is the transformation $\langle\text{out}_\pm| \rightarrow \langle\text{out}_\pm|B$, i.e. $\langle\text{out}_\pm|$ must be charged under the gauge symmetry.

The MBQC protocol on a ring With respect to the adaptive eigenbasis of $O((-)^{q_j}\alpha_j)$, the wavefunction for the cluster state is given by

$$|1\rangle = \mathcal{N} \sum_{g_j \in \mathbb{Z}_2 \times \mathbb{Z}_2} \text{Tr}(B_{g_N \dots g_1} U) |g_N\rangle \cdots |g_2\rangle |g_1\rangle, \quad (3.20)$$

where $|g\rangle$ are adapted basis elements as defined in (3.7), and we have applied equation (2.23). We now observe that any $SU(2)$ matrix U can be expanded in the operator basis V_g as

$$U = \sum_g c_g V_g \quad (3.21)$$

The coefficients in this expansion are:

$$c_g = \text{Tr}(V_g^\dagger U) / \text{Tr}(V_g^\dagger V_g) = \frac{1}{2} \text{Tr}(V_g^\dagger U) \quad (3.22)$$

Since B takes values in $V_g = \pm V_g^\dagger$, the amplitudes $\text{Tr}(B U)$ determine the coefficients c_g up a phase.

The MBQC protocol on a ring returns as computational output the probability distribution $p_g = |c_g|^2$. As anticipated, the reported data consist of two classical bits of information. They fully characterize the simulated unitary $U \in SU(2)$ as an expansion in the operator basis V_g . In the end, the output is sensitive only to the overall byproduct operator (2.24), which accumulates around the ring.

In the next section, we interpret the byproduct B as a Wilson loop of a $\mathbb{Z}_2 \times \mathbb{Z}_2$ gauge field or, equivalently, as a $\mathbb{Z}_2 \times \mathbb{Z}_2$ flux. In terms of individual measurement outcomes s_j , the

computational output is the $\mathbb{Z}_2 \times \mathbb{Z}_2$ -valued random variable:

$$o = \prod_j g_j \quad (3.23)$$

Once more, we emphasize that (3.23) puts all measurement outcomes on equal footing.

For future reference, notice that the adaptation of measurement angles on the ring can again be understood in terms of stabilizer transformations, just as it could on the chain. In particular, equations (3.18), which generate the globally adapted basis, leave the computational output invariant. One simplification on the ring is that the corrective procedure involves only $K_j = Z_{j+1}X_jZ_{j-1}$; there are no more special stabilizers such as $X_{2N+1}Z_{2N}$.

4 The gauge theory of MBQC

In this section, we establish the gauge theory of MBQC. In Section 4.1, we describe the MBQC gauge principle, first informally and then formally as a theorem. This invokes centrally a notion of ‘reference.’ The mathematics of gauge theory knows of such an object—the section. This correspondence forms the starting point for reviewing the mathematical underpinning of gauge theory in Section 4.2. There we establish how the notion of gauge potential applies to MBQC. With this insight, we re-examine the classical side processing relations of MBQC in Section 4.4.

4.1 Gauge principle

In the circuit interpretation of MBQC, individual quantum gates can only be implemented up to a byproduct operator in the Pauli group. The byproduct operator is a priori random but known through the outcome of the measurement that implemented the gate. That is, if U_i is the intended gate, then in any given run of the MBQC, any of the four gates in the equivalence class

$$[U_i] = \{U_i, X U_i, Y U_i, Z U_i\}. \quad (4.1)$$

may be implemented, depending on the measurement outcome s_i on block i . Thus, the procedure of gate simulation is one and the same for the entire class $[U_i]$. The in-advance unpredictable measurement result is picked by a whim of nature, and it determines the representative.

Likewise, the person operating an MBQC may choose a representative of $[U_i]$ as the operation intended. Different choices of target within the class $[U_i]$ are equivalent, because the implementation procedure can aim for the class only. Picking the intended operation is therefore a choice of reference. In the following we denote it as $U_{f_i} \in [U_i]$, keeping in mind that there is one choice f_i per block i ; i.e. the total gauge choice is $\mathbf{f} = (f_1, \dots, f_N)$.

The gauge theory formulation of MBQC developed here is based on the following observation:

MBQC gauge principle. For any given MBQC, the reference \mathbf{f} can be changed without changing the quantum computation. The changes in the reference \mathbf{f} are the MBQC gauge transformations.

The principle says that an external observer of a measurement-based quantum computation who has access to the measurement record, the measurement bases, and the computational output, and who furthermore knows what the computational task is, can not infer which gauge-equivalent reference \mathbf{f} is used by the operator of the MBQC.

4.1.1 Formulating the MBQC gauge principle as a theorem

Since the framework of MBQC already exists, the MBQC gauge principle cannot just be postulated. Rather it arises as a theorem. We establish it here for measurement-based quantum computations on 1D cluster states, as the simplest instance. Beyond 1D cluster states, we establish it for the entire $\mathbb{Z}_2 \times \mathbb{Z}_2$ SPT phase surrounding the 1D cluster state in Section 5.6. We conjecture the MBQC gauge principle to hold for cluster states in arbitrary dimension, and for subsystem SPT phases surrounding them.

In the review of MBQC in Section 2, and indeed in the exploration of MBQC to date, the concept of the reference \mathbf{f} has not been identified. Implicitly, the choice $\mathbf{f} = 0$ has always been assumed. This is not the only admissible choice of reference, and structural information about MBQC is revealed by realizing that this is so.

We now formulate the gauge principle at the level of the MPS tensors representing the cluster state in the MBQC measurement basis. We do this in two stages. First, we consider individual MPS matrices in isolation, which conveys the general idea. In a second step, we consider all the MPS matrices (one per block) in combination, as they are linked through the adaptation of measurement bases in MBQC. This leads us to the explicit form of the gauge transformation in Lemma 2 below.

Single block level. Let us focus on a single MPS tensor and denote the physical measurement outcomes (two bits' worth) at the i^{th} block as s_i . Denoting the reference for block i by f_i , we consider measurements in the locally adapted basis $|s_i\rangle = l(g_i)|f_i\rangle$ as in eq. (3.6). Projected onto this basis, the MPS tensor decomposes as

$$A_{s_i} = V_{g_i} U_{f_i},$$

with $U_{f_i} := A_{f_i}$ the ‘intended gate,’ and V_{g_i} the outcome-dependent Pauli byproduct. We observe that the different components of the MPS tensor A of the cluster state differ only by Pauli operators. As shown in Figure 6, this is a special property of the cluster tensor implied by its transformation law under the symmetry $l(\mathbb{Z}_2 \times \mathbb{Z}_2)$.

At this point, we realize that the splitting into an outcome-dependent Pauli part V_g and an outcome-independent unitary U_f is not unique. In particular, we are not required to

take $f_i = (+_{\alpha_{2i}} +_{\alpha_{2i-1}})$ as the reference outcome; any outcome f will do. Under a change of reference

$$|\tilde{f}_i\rangle := l(h_i) |f_i\rangle, \quad \tilde{g}_i = g_i h^{-1}, \quad (4.2)$$

we may write

$$|s_i\rangle = l(g_i) |f_i\rangle = l(\tilde{g}_i) |\tilde{f}_i\rangle, \quad \forall i = 1, \dots, N, \quad (4.3)$$

so the group label for $|s_i\rangle$ changes to \tilde{g}_i . Each component A_s of the MPS tensor A may now be written as

$$A_{s_i} = V_{g_i} U_{f_i} = V_{\tilde{g}_i} U_{\tilde{f}_i}. \quad (4.4)$$

For any Pauli operator $V_h \in \mathcal{P}_1$, the mapping $U_f \mapsto U_{\tilde{f}_i} = V_h U_{f_i}$, $V_{g_i} \mapsto V_{\tilde{g}_i} = V_{g_i} V_h^\dagger$ keeps A_{s_i} invariant; and furthermore $V_h U_{f_i} \in SU(2)$ for all $U_{f_i} \in SU(2)$, and $V_{s_i} V_h^\dagger \in \mathcal{P}_1$ for all $V_{s_i} \in \mathcal{P}_1$. The splitting of A_{s_i} into an outcome-dependent Pauli part V_{s_i} and an outcome-independent general unitary part U_{f_i} is therefore ambiguous. This ambiguity is the origin of the MBQC gauge principle.

Gauge dependence at the multi-block level. The reason we need to look at multiple MPS matrices combined is the adaptivity of local measurement basis in MBQC, according to previously obtained measurement outcomes. This is captured by equation (3.12), where the outcome dependence of the measurement basis at block i is implemented by $u(g_{\prec i})$. Since $u(g_{\prec i})$ depends on the group labels $g_j, j \leq i$, the basis states $|g_i\rangle$ transform nontrivially under a change of reference on any site $j \leq i$. Likewise the MPS tensor A_{g_i} measured in the adapted basis depends on reference choices on sites $j \leq i$. To make explicit the dependence of MBQC on change of references, let us introduce reference labels on the globally adapted basis states and the corresponding MPS tensors :

$$\begin{aligned} |g_i\rangle &:= |g_i, f_i\rangle = l(g_i) u(g_{\prec i}) |f_i\rangle \\ A_{g_i} &:= A_{g_i, f_i} = V_{g_{\prec i}} (V_{g_i} U_{f_i}) V_{g_{\prec i}}^\dagger \end{aligned} \quad (4.5)$$

Similarly, classical side processing data depend on the reference via their explicit dependence on group labels:

$$(q_{2i}, q_{2i-1}) = g_{\prec i} \quad (\text{as element of } \mathbb{Z}_2 \times \mathbb{Z}_2) \quad (4.6)$$

$$o = \prod_i g_i \quad (4.7)$$

If we define

$$A_{\mathbf{g},\mathbf{f}} = \prod_i A_{g_i,f_i}, \quad V_o = \prod_i V_{g_i}, \quad U_{\mathbf{f}} = \prod_i U_{f_i}, \quad (4.8)$$

the total MPS wavefunction for the cluster chain is given by

$$A_{\mathbf{g},\mathbf{f}} = V_o U_{\mathbf{f}} \quad (4.9)$$

where we have used byproduct propagation to obtain the RHS as in equation (2.23).

Equations (4.5-4.9) summarize all the relevant formulas of MBQC. Inspection of these relations motivates a further constraint to impose on the change of reference. From the circuit model perspective, $U_{\mathbf{f}}$ is the unitary that MBQC realizes and to which the classical output of MBQC refers; i.e. the MBQC output reveals properties of $U_{\mathbf{f}}$. The change of reference should not change that interpretation. Thus, while the locally implemented pieces U_{f_i} may change under the gauge transformation, their cumulative product $U_{\mathbf{f}}$ should not.

We thus arrive at the following definition for the notion of MBQC gauge transformations.

Definition 1. *An MBQC gauge transformation is a change of reference $|\mathbf{f}\rangle \mapsto |\tilde{\mathbf{f}}\rangle$ and accompanying change of the group labels for the byproducts $\mathbf{g} = (g_1, \dots, g_N)$ such that (i) all MPS matrices A_{g_i,f_i} are preserved, up to possible global phases, and (ii) the total MBQC-implemented unitary is preserved,*

$$U_{\mathbf{f}} \mapsto U_{\tilde{\mathbf{f}}} = U_{\mathbf{f}}. \quad (4.10)$$

In a different terminology, the gauge transformations defined above are called proper gauge transformations whereas changes of reference that satisfy condition (i) but do not satisfy (ii) are called ‘large’ gauge transformations.

Eq. (4.9), in combination with Definition 1, leads to the following observation:

Lemma 1. *The cumulative MPS matrix $A_{\mathbf{g},\mathbf{f}}$, the target unitary $U_{\mathbf{f}}$ and the cumulative byproduct V_o are, up to possible global phases, invariant under the MBQC gauge transformations.*

Proof of Lemma 1. $A_{\mathbf{g},\mathbf{f}}$ and $U_{\mathbf{f}}$ are invariant by Definition 1. Therefore, by Eq. (4.9), the cumulative byproduct V_o is also invariant. \square

We now provide an explicit construction of the gauge transformations according to Definition 1. We have the following result:

Lemma 2. *For all $i = 1, \dots, N - 1$ and all $h \in \mathbb{Z}_2 \times \mathbb{Z}_2$, the transformations $h^{(i)}$ defined by*

$$\begin{aligned} U_{f_i} &\mapsto U_{\tilde{f}_i} = V_h U_{f_i}, & V_{g_i} &\mapsto V_{\tilde{g}_i} = V_{g_i} V_h^\dagger, \\ U_{f_{i+1}} &\mapsto U_{\tilde{f}_{i+1}} = U_{f_{i+1}} V_h^\dagger, & V_{g_{i+1}} &\mapsto V_{\tilde{g}_{i+1}} = V_{g_{i+1}} V_h. \end{aligned} \quad (4.11)$$

are MBQC gauge transformations.

The gauge transformations Eq. (4.11), together with the equivariant transformations $l(\cdot)$ and $r(\cdot)$ of the cluster state MPS tensor displayed in Figure 5, imply the following transformation on the reference $|\mathbf{f}\rangle$:

$$h^{(i)} : |f_i\rangle \mapsto l(h) |f_i\rangle, |f_{i+1}\rangle \mapsto r(h) |f_{i+1}\rangle, \quad (4.12)$$

with all other components of \mathbf{f} unchanged. The corresponding change in group labels is:

$$\tilde{g}_i = g_i h^{-1}, \quad \tilde{g}_{i+1} = h g_{i+1}. \quad (4.13)$$

Proof of Lemma 2. We have to check that the transformations according to eq. (4.11) satisfy Properties (i) and (ii) of Definition 1.

Property (i). The gauge transformation (4.11), for any fixed i , affects non-trivially only blocks i and $i + 1$. Checking the corresponding MPS matrices, we find:

$$\begin{aligned} A_{g_i, f_i} &= V_{g_{\prec i}} (V_{g_i} U_{f_i}) V_{g_{\prec i}}^\dagger \\ &\mapsto V_{\tilde{g}_{\prec i}} \left(V_{\tilde{g}_i} U_{\tilde{f}_i} \right) V_{\tilde{g}_{\prec i}}^\dagger \\ &\propto V_{g_{\prec i}} \left(V_{g_i} V_h^\dagger V_h U_{f_i} \right) V_{g_{\prec i}}^\dagger \\ &= V_{g_{\prec i}} (V_{g_i} U_{f_i}) V_{g_{\prec i}}^\dagger \\ &= A_{g_i, f_i}, \end{aligned}$$

and

$$\begin{aligned} A_{g_{i+1}, f_{i+1}} &= V_{g_{\prec i+1}} (V_{g_{i+1}} U_{f_{i+1}}) V_{g_{\prec i+1}}^\dagger \\ &\mapsto V_{\tilde{g}_{\prec i+1}} \left(V_{\tilde{g}_{i+1}} U_{\tilde{f}_{i+1}} \right) V_{\tilde{g}_{\prec i+1}}^\dagger \\ &\propto V_{g_{\prec i+1}} V_h^\dagger \left(V_{g_{i+1}} V_h U_{f_{i+1}} V_h^\dagger \right) V_h V_{g_{\prec i+1}}^\dagger \\ &\propto V_{g_{\prec i+1}} (V_{g_{i+1}} U_{f_{i+1}}) V_{g_{\prec i+1}}^\dagger \\ &= A_{g_{i+1}, f_{i+1}}. \end{aligned}$$

Thus, up to possible global phases, the MPS matrices are invariant. Property (i) is satisfied.

Property (ii). Using (4.11), we have:

$$\begin{aligned} U_{\mathbf{f}} &= U_{f_N} \dots U_{f_{i+2}} U_{f_{i+1}} U_{f_i} U_{f_{i-1}} \dots U_{f_1} \\ &\mapsto U_{f_N} \dots U_{f_{i+2}} \left(U_{f_{i+1}} V_h^\dagger \right) (V_h U_{f_i}) U_{f_{i-1}} \dots U_{f_1} \\ &= U_{f_N} \dots U_{f_{i+2}} U_{f_{i+1}} U_{f_i} U_{f_{i-1}} \dots U_{f_1} \\ &= U_{\mathbf{f}}. \end{aligned}$$

Thus, Property (ii) holds as well. \square

We can now state the MBQC gauge principle as a theorem:

Theorem 1 (MBQC gauge principle). *For any given MBQC on 1D cluster states, the measurement bases $\{|g_i, f_i\rangle\}$ chosen as a function of prior measurement record $g_{\prec i}$, the output o*

given the measurement record \mathbf{g} , and the probability distribution of the computational output o , $p(o) = |\text{Tr}(U_{\mathbf{f}}V_o)|^2$, are invariant under gauge transformations (4.11-4.13).

This has the following consequence: An external observer, who tracks an MBQC computation and has access to all measurement settings, the measurement record and the computational output, cannot infer which reference \mathbf{f} is used in the internal classical side processing.

Proof of Theorem 1. (i) The local measurement bases: Under the gauge transformation $h^{(i)}$, the local measurement basis $\{|g_{i+1}, f_{i+1}\rangle, g_{i+1} \in \mathbb{Z}_2 \times \mathbb{Z}_2\}$ at block $i+1$ transforms as:

$$\begin{aligned}
l(g_{i+1})u(g_{\prec i+1})|f_{i+1}\rangle &\rightarrow l(\tilde{g}_{i+1})u(\tilde{g}_{\prec i+1})|\tilde{f}_{i+1}\rangle \\
&= l(hg_{i+1})u(g_{\prec i+1})u(h)r(h)|f_{i+1}\rangle \\
&= l(g_{i+1}h)u(g_{\prec i+1})l(h)|f_{i+1}\rangle \\
&\propto l(g_{i+1}h)l(h)u(g_{\prec i+1})|f_{i+1}\rangle \\
&= l(g_{i+1})u(g_{\prec i+1})|f_{i+1}\rangle
\end{aligned} \tag{4.14}$$

In the first line, we have used the gauge transformations (4.12-4.13). In the third line we have used $u(h) = l(h)r(h)$, cf. eq. (3.3), and in the fourth we commuted $u(g_{\prec i+1})$, and $l(h)$ at the cost of an irrelevant sign. We thus find that the measurement basis for block $i+1$ is indeed invariant under the gauge transformations $h^{(i)}$.

On the i^{th} block, we have:

$$\begin{aligned}
l(g_i)u(g_{\prec i})|f_i\rangle &\rightarrow l(\tilde{g}_i)u(\tilde{g}_{\prec i})|\tilde{f}_i\rangle \\
&= l(g_ih)u(g_{\prec i})l(h)|f_i\rangle \\
&\propto l(g_ih)l(h)u(g_{\prec i})|f_i\rangle \\
&\propto l(g_i)u(g_{\prec i})|f_i\rangle
\end{aligned} \tag{4.15}$$

On all other blocks, the gauge transformation $h^{(i)}$ acts trivially. Thus, all local measurement bases are gauge-invariant.

(ii) Single-shot computational output o : A gauge transformation $h^{(i)}$ transforms the computational output as follows:

$$\begin{aligned}
o &= g_1 \dots g_N \\
&\mapsto g_1 \dots g_{i-1} (g_i h^{-1}) (h g_{i+1}) g_{i+2} \dots g_N \\
&= g_1 \dots g_N \\
&= o.
\end{aligned}$$

Thus, the output o is invariant under $h^{(i)}$, for any $h \in \mathbb{Z}_2 \times \mathbb{Z}_2$, for any i .

(iii) Output statistics: Since o is gauge invariant per item (ii), so is V_o , up to a possible phase. $U_{\mathbf{f}}$ is invariant by assumption; cf. eq. (4.10). Therefore $p(o) = |\text{Tr}(U_{\mathbf{f}}V_o)|^2$ is gauge-invariant. \square

4.2 Mathematical underpinning of gauge theory

We now formalize the objects encountered in Section 4.1. Our first goal is to review the concept of ‘section,’ and, for the application to MBQC, identify it with the reference \mathbf{f} .

4.2.1 Fiber bundles, sections, and gauge transformations

Gauge theory is a theory of fiber bundles. Accordingly, our next step is to present a (discrete) fiber bundle, which describes the geometry of an MBQC computation. We begin with a lightning review of fiber bundles.

A fiber bundle is a family of identical spaces (fibers) F_b , which are labeled by elements of another topological space $\mathcal{B} \ni b$, called the base space. The union of all fibers is called ‘total space’ and denoted \mathcal{E} :

$$\mathcal{E} = \bigcup_{b \in \mathcal{B}} F_b \quad (4.16)$$

Locally, any fiber bundle looks like the direct product $F \times \mathcal{B}$. Globally, however, the direct product structure breaks down because the different fibers can be arranged over \mathcal{B} in a nontrivial way. Common examples of nontrivial bundles include the Möbius strip, in which the interval $[0, 1] =: F_b$ gets reflected as b goes around the circle $S^1 =: \mathcal{B}$, or the tangent spaces $T_b =: F_b$ over a manifold $\mathcal{M} =: \mathcal{B}$ if the manifold is curved.

It is useful to distinguish two types of bundles. First, a principal fiber bundle \mathcal{G} , also called a gauge bundle, has as fibers copies of a symmetry group G . Given a gauge bundle and a choice of representation R , we can define an associated vector bundle \mathcal{V}_R whose fibers are the vector spaces on which the representation R acts. In the conventional setting of continuum gauge theory, \mathcal{V}_R corresponds to a choice of matter field transforming in the representation R . The gauge field then couples to this matter field via covariant derivatives in the chosen representation.

The MBQC gauge bundle The structure of the MBQC gauge bundle is manifest in the MPS description of the resource state. The base space \mathcal{B} is the one-dimensional lattice where the physical qubits live. In the cluster state, due to the symmetries of the MPS tensor, we will identify a single point $j \in \mathcal{B}$ with a block of two physical qubits.

The fiber above each block is the group $\mathbb{Z}_2 \times \mathbb{Z}_2$, which permutes the four possible measurement outcomes. Equivalently, each fiber of the MBQC gauge bundle consists of the measurement outcomes themselves. We anticipated this in equation (3.7) when we labeled measurement outcomes with group elements.

As emphasized above that equation, a labeling of a fiber with group elements is not unique since we can always act with the group on itself and get a new labeling. To coordinatize a fiber with group elements, we must therefore choose a so-called section²: an outcome in every fiber, which is labeled with the identity element of the group. We did that in equation (3.7) by

²In a general fiber bundle there may not exist a global section, but this subtlety does not arise in this paper.

choosing the outcome $(s_{2j}, s_{2j-1}) = (0, 0)$ —equivalently, the basis vector $|+\alpha_{2j}\rangle \otimes |+\alpha_{2j-1}\rangle$ —as a reference. Note that, from the MBQC programmer’s point of view, the identification of the state $|+\alpha_{2j}\rangle \otimes |+\alpha_{2j-1}\rangle$ with the group element $++ \in \mathbb{Z}_2 \times \mathbb{Z}_2$ is an arbitrary choice. Other measurement outcomes can be identified with the identity element equally well. To maintain the visual correspondence between measured states $|\pm(\dots)\rangle$ and group elements, the programmer can always modify the reference measurement angles, for example:

$$| -(-\alpha_2) \rangle \otimes | -\alpha_1 \rangle = | +(\pi-\alpha_2) \rangle \otimes | +(\pi+\alpha_1) \rangle \quad (4.17)$$

More formally, a section is one choice of element in each fiber:

$$f: \mathcal{B} \rightarrow \mathcal{E} \quad \text{such that } j \rightarrow f_j \in F_j \quad (4.18)$$

In MBQC, we identify the set of reference outcomes \mathbf{f} with a section f of the gauge bundle.

A gauge transformation h is a map that relates two sections f_j and \tilde{f}_j :

$$h: \mathcal{B} \rightarrow G \quad \text{such that } j \rightarrow h_j \quad \text{with } \tilde{f}_j = h_j f_j \quad (4.19)$$

This is depicted in the right of Figure 8.

Note the subtle difference between a section and a gauge transformation. The former maps \mathcal{B} to the fibers while the latter maps \mathcal{B} directly to the group. This is because $h_j = \tilde{f}_j f_j^{-1}$ is a relative construct, from which the ambiguity in labeling fibers cancels out.

The associated bundle The associated bundle \mathcal{V}_R for MBQC has the same base space as the gauge bundle, but the fibers are replaced by the virtual Hilbert space, which transforms under the projective representation of $\mathbb{Z}_2 \times \mathbb{Z}_2$. More specifically, we define F_j on the j^{th} block to be the Hilbert space on the left virtual edge of the MPS tensor. A gauge transformation h_j acts on the associated bundle via the projective representation V_{h_j} , which rotates each fiber of \mathcal{V}_R . The virtual qubit in the circuit simulation thus plays the role of the ‘matter field’ in the analogy with ordinary field theory.

4.2.2 Parallel transport

A key concept in the study of fiber bundles is parallel transport. It sets a convention for what it means for a trajectory in the total space \mathcal{E} to travel entirely in a ‘horizontal direction,’ with no component of motion in the fiber. (In this nomenclature, motion over one point j in the base space—that is entirely within F_j —is ‘vertical.’) Without a definition of parallel transport there is no canonical way of comparing fibers over different base points. Parallel transport relates different fibers to one another in a definite, albeit non-canonical, way. It is specified by a linear map between adjacent fibers F_{j-1} and F_j . In MBQC, parallel transport is generated by the MPS tensor $A_{s_j} = A_{s_j}((-)^{q_{2j}}\alpha_{2j}, (-)^{q_{2j-1}}\alpha_{2j-1})$ in the adapted basis:

$$A_{s_j} : F_{j-1} \rightarrow F_j, \quad (4.20)$$

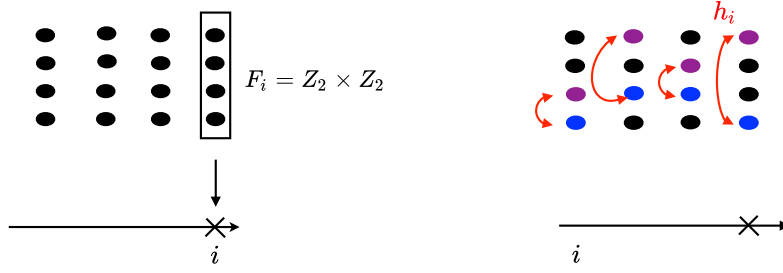


Figure 8: The MBQC gauge bundle is defined by the action of the $\mathbb{Z}_2 \times \mathbb{Z}_2$ transformations $l_i(g)$ on the measurement outcomes. The orbits form the fiber $\{f_i\}$ over a block, which is just a copy of $\mathbb{Z}_2 \times \mathbb{Z}_2$. The purple and blue dots describe two sections of this bundle, corresponding to two sets of measurement outcomes. The sections are related by a gauge transformation, denoted by h_i .

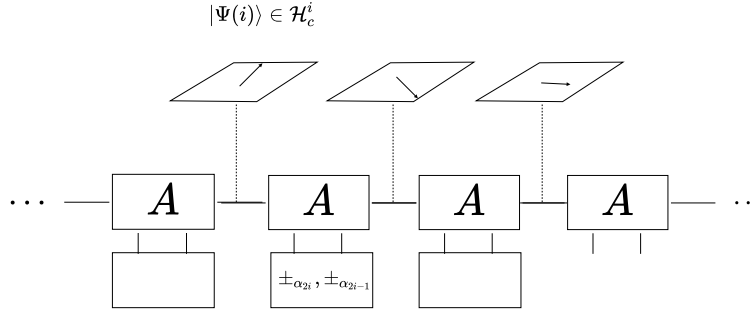


Figure 9: The fibers $F_i = \mathcal{H}_c^i$ of the vector bundle \mathcal{V} are copies of the virtual Hilbert space where the virtual qubit lives.

We thus identify parallel transport on the bundle \mathcal{V}_R with the quantum teleportation of the virtual qubit. In MBQC, parallel transport is induced by measurements. Prior to a measurement, the definition of parallel transport is fluctuating; we called this circumstance a fluctuating circuit in Section 2.1. Measurements in the MBQC basis force parallel transport to take on a definite, classical form.

Gauge connection The generator of local parallel transport A_s is a gauge invariant linear map describing a horizontal motion between neighboring fibers. It is independent of the group label assigned to the measurement outcome s . On the other hand, the gauge connection describes a gauge dependent motion along F_i that depends on a choice of section. To determine the MBQC gauge connection, recall that a choice of section provides a group

label for the measurement outcome s according to

$$s = gf = \tilde{g}\tilde{f} \quad (4.21)$$

We think of s as an element of the fiber F_j in the gauge bundle, which has coordinates g and \tilde{g} relative to two reference sections f and \tilde{f} . Using the relation (3.9), we can write the parallel transport as

$$A_s = V_g U_f = V_{\tilde{g}} U_{\tilde{f}}, \quad (4.22)$$

where we used the notation $U_f = A_f$ to emphasize that A_f is the (desired) local circuit simulation.

Equation (4.22) shows that a gauge choice decomposes the parallel transport operator into two parts. The first is a ‘naïve motion’ U_f , which can contain both horizontal and vertical motion. In the total space \mathcal{E} , this naïve motion simply follows the section f . The second part, V_g , is the gauge connection. It is a correction term, whose action is entirely vertical—that is, it maps the fiber to itself. Its job is ensure that the combination $V_g U_f$ generates parallel transport. Note that, when viewed in isolation, both V_g and U_f are ambiguous up to multiplication by V_h for arbitrary h in the gauge group; only their product has invariant meaning. This is the gauge symmetry of MBQC: the freedom to reset the section f and the corresponding ambiguity in the byproduct V_g .

Parallel transport in the globally adapted basis The MPS tensor A_s in equation (4.22) describes the evolution a virtual qubit $|\psi\rangle$ in the locally adapted basis defined in (3.6). Measurements in that basis produce the virtual evolution

$$|\psi\rangle \rightarrow \cdots V_{g_i} U_{f_i} \cdots V_{g_1} U_{f_1} |\psi\rangle \quad (4.23)$$

However, MBQC involves measurement in a globally adapted basis, in which the MPS tensor A_{s_i} is conjugated by the byproduct operator $V_{g_{\prec i}}$ as in (3.15). Naïvely, the virtual evolution is more complicated, but if propagate the byproducts as described in Section 2, we again get a simple form of the virtual evolution:

$$|\psi\rangle \rightarrow (\cdots V_{g_2} V_{g_1}) (\cdots U_{f_2} U_{f_1}) |\psi\rangle \quad (4.24)$$

Thus, after the i^{th} measurement, we can interpret $(\prod_{j \leq i} V_j)(\prod_{j \leq i} U_{f_j})$ as total parallel transport, expressed as a combination of the ‘naïve’ motion $(\prod_{j \leq i} U_{f_j})$ and a correction $(\prod_{j \leq i} V_j)$.

Gauge connection on the principal bundle We can also define a gauge connection directly on the gauge bundle \mathcal{G} . Given a history of measurement outcomes

$$s_j = g_j f_j \quad j = 1, \dots, N \quad (4.25)$$

and a gauge choice f , we define the connection on the gauge bundle to be $\mathbf{g} = (g_1, \dots, g_N)$. Thus, the measurement record, labelled by a set of elements of $\mathbb{Z}_2 \times \mathbb{Z}_2$, is the MBQC gauge field! This is because the connection on the vector bundle is V_{g_j} and the two bundles are related to one another by the representation map. Furthermore, we can define the gauge potential at block j as the pair of binary numbers $\vec{a}_j = (a_{j:1}, a_{j:2})$ satisfying:

$$g_j = ((-1)^{a_{j:1}}, (-1)^{a_{j:2}}) \quad (4.26)$$

Thus, the gauge potential is just a $\mathbb{Z}_2 \times \mathbb{Z}_2$ variable like g_j , written in additive notation.

4.3 Holonomies and fluxes

Observables in gauge theory are fluxes through closed loops. In mathematical terms, a (classical) flux corresponds to a property of a fiber bundle called holonomy. It is computed by the product of parallel transport generators around a given loop:

$$\text{flux} \leftrightarrow \text{holonomy} = \prod_{\text{loop}} (\text{parallel transport}) \quad (4.27)$$

This formula is illustrated in Figure 10. As reviewed in the previous subsection, parallel transport is a map from one fiber to another: $F_j \rightarrow F_{j+1}$. A composition of parallel transport around a closed loop therefore gives a transformation of the initial fiber to itself:

$$\text{holonomy} : F_1 \rightarrow F_1 \quad (4.28)$$

Geometrically, this transformation tells us whether (and how) a fiber bundle is ‘twisted.’ In the present context, where fibers are labeled by group elements, we expect four distinct holonomies that send $|g\rangle \in F_1$ to $|hg\rangle \in F_1$, where $h \in \mathbb{Z}_2 \times \mathbb{Z}_2$. Physically, the ‘twisting’ of the fiber bundle is interpreted as a classical value of flux.

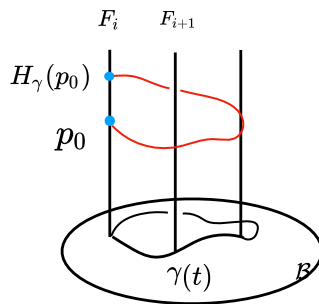


Figure 10: A holonomy H_γ on the *principal* fiber bundle is defined by lifting a curve $\gamma(t)$ from the base space to the total space. Given a section, this curve is a choice of group element g_i at each fiber describing local parallel transport, which combines into a holonomy $o = \prod_i g_i$.

Physical flux Substituting the definition of parallel transport in (4.20) and equation (4.24), we get:

$$\text{flux} = \prod_{j=1}^N A_{g_j, f_j} = \left(\prod_{j=1}^N V_{g_j} \right) \left(\prod_{j=1}^N U_{f_j} \right) = V_o U_{\text{total}} \quad (4.29)$$

This is the flux after a complete set of MBQC measurements, which force the fluctuating parallel transport operators to take on definite values A_{g_j, f_j} .

Equation (4.29) does not correspond to any one element h of $\mathbb{Z}_2 \times \mathbb{Z}_2$, so how to interpret this equation? We view it as a quantum mechanical superposition of fluxes. To do so, expand

$$U_{\text{total}} = \sum_{g \in \mathbb{Z}_2 \times \mathbb{Z}_2} c_g V_g \quad (4.30)$$

in the V_g , which form a complete basis in the space of $SU(2)$ matrices. Then equation (4.29) becomes:

$$\text{flux} = \sum_{g \in \mathbb{Z}_2 \times \mathbb{Z}_2} c_g b(o, g) V_{o \cdot g}, \quad (4.31)$$

where the projective phases $b(o, g)$ are defined by $V_o V_g = b(o, g) V_{o \cdot g}$ (These are never observed in MBQC). The right hand side is a linear combination of the four classically allowed holonomies $o \cdot g \in \mathbb{Z}_2 \times \mathbb{Z}_2$.

Since classical fluxes correspond to differently twisted bundles, states of a quantum gauge theory naturally describe superpositions of distinct bundles. A special case of (4.31) occurs

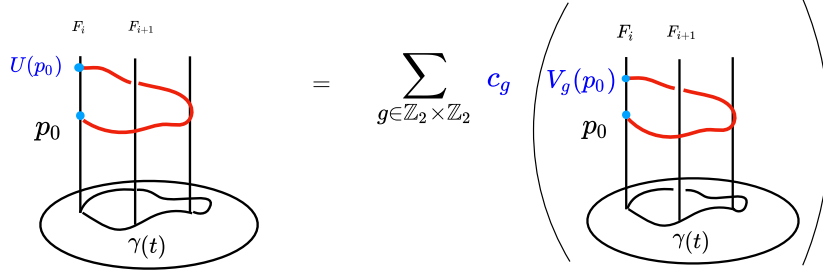


Figure 11: This figure illustrates the superposition of vector bundles \mathcal{V}_g with holonomy V_g . In contrast with the gauge bundle where the fibers are copies of the gauge group, the fibers of \mathcal{V}_g are virtual Hilbert spaces \mathbb{C}^2 where the virtual qubit lives. On the right, each term in the sum describes the parallel transport of an element $p_0 \in \mathbb{C}^2$ around a closed loop, which transforms p_0 by a holonomy matrix V_g . MBQC superposes such holonomies to obtain a general $SU(2)$ transformation U , which gives the simulated unitary.

in an MBQC simulation of $U_{\text{total}} = 1$ or a Pauli matrix. In this circumstance the superposition (4.31) involves a single term with $o \cdot g = ++ \in \mathbb{Z}_2 \times \mathbb{Z}_2$, so the outcome o of MBQC is deterministic. We can understand such deterministic MBQC as measuring the trivial flux

of the initial resource state $|1\rangle$. Non-deterministic MBQC, in contrast, projects the resource state onto superpositions of fluxes, which are defined in equation (4.31). We examine those states, and explain MBQC as a flux measurement in a non-diagonal basis, in Section 5.4.

MBQC flux Consider one MBQC run, during which the resource state gets projected onto a superposition of fluxes defined in equation (4.31). The MBQC technician records the computational outcome

$$o = g_N \dots g_2 g_1 \in \mathbb{Z}_2 \times \mathbb{Z}_2 \quad (4.32)$$

where $V_o = B$ from equation (2.23). From the technician’s perspective, it is tedious and pedantic to say that she has projected the resource state onto a superposition of flux states; identifying flux with o directly is equally informative but far simpler.

In the remainder of the paper, we refer to $o \in \mathbb{Z}_2 \times \mathbb{Z}_2$ as ‘MBQC flux.’ Notice that MBQC fluxes could be made consistent with equation (4.27) if we identified ‘MBQC parallel transport’ with the individual measurement outcomes $g_j \in \mathbb{Z}_2 \times \mathbb{Z}_2$:

$$\text{‘MBQC parallel transport’} = g_j \text{ measured on the } j^{\text{th}} \text{ block} \quad (4.33)$$

As we presently explain, this definition depends on subjective intentions of the MBQC technician. This is why it is useful to distinguish MBQC flux and ‘MBQC parallel transport’ from their physical counterparts: only the latter are free of teleological considerations.

MBQC flux versus physical flux Consider a run of deterministic MBQC, in which every qubit is measured in the X -basis. Two quantum programmers, Alice and Bob, observe the run and jot down all measurement outcomes. Whereas Alice intends to use this MBQC run as a simulation of $U_{\text{total}}^{\text{Alice}} = 1 = V_{++}$, Bob intends to simulate $U_{\text{total}}^{\text{Bob}} = X = V_{+-}$. We observed previously that the outcome o of deterministic MBQC satisfies $o \cdot g = ++$, where the simulated unitary is $U_{\text{total}} = V_g$. Therefore, Alice reports MBQC flux $o^{\text{Alice}} = ++$ whereas Bob reports MBQC flux $o^{\text{Bob}} = +-$. Their MBQC fluxes differ even though they are describing the same physical experiment.

Physical fluxes defined by equation (4.29) do not suffer from this teleological ambivalence. On the other hand, it is the MBQC fluxes that constitute the computational output o . With a fixed choice of the simulated U_{total} , going from the physical fluxes to MBQC fluxes is a simple change of basis described by equation (4.31). We can already see—and we will explain in more detail in Section 5.4—that MBQC proceeds by projecting states of definite physical flux (such as the cluster state) onto states of definite MBQC flux.

Analogy It is useful to compare the definitions of flux (both physical and MBQC) with more familiar gauge theories such as electromagnetism. In $U(1)$ gauge theory, the Aharonov-Bohm effect relates the flux of a magnetic field through a loop to the additional phase incurred by a charged particle that circles that loop:

$$\text{flux} \propto \exp \oint D_\mu dx^\mu = \exp \oint A_\mu dx^\mu \in U(1) \quad (4.34)$$

Written in this form, the flux is also known as a Wilson loop. The object $D_\mu = \partial_\mu + A_\mu$ is the covariant derivative, which generates parallel transport in the underlying $U(1)$ fiber bundle. In more technical language, D_μ is the Ehrenfest connection—the generator of parallel transport acting in the total space \mathcal{E} . It is the action of D_μ , which is pictured in red in Figure 10.

The object A_μ is what physicists call the gauge potential. As emphasized before, it is defined relative to a section f , which is a map from the base to the fibers. The equality of the two integrals in (4.34) follows from the assumed single-valuedness of f . The two integrands differ by pure coordinate transport $\partial_\mu = D_\mu - A_\mu$ in the base, which lifts in total space to following the section f . When the section is single-valued, a closed loop in the base lifts to a closed loop in total space and explicitly including ∂_μ in (4.34) becomes immaterial.

The situation is different when we contemplate a choice of ‘section,’ which is not single-valued. In that circumstance, a closed loop in the base lifts to a non-trivial transformation on the fiber

$$U_{\text{section}} : f_{\text{initial}} \rightarrow f_{\text{final}} \quad (4.35)$$

and equation (4.34) becomes modified:

$$\text{flux} \propto \exp \oint D_\mu dx^\mu = \exp \oint A_\mu dx^\mu \times U_{\text{section}} \in U(1) \quad (4.36)$$

This relation is directly analogous to equation (4.29), which relates the physical and MBQC flux. Parallel transport defined in (4.20) plays the role of the covariant derivative D_μ in continuum gauge theory. The role of the gauge potential³ is played by the measurement outcomes g_j (in the gauge bundle \mathcal{G}) or by their representations matrices V_{g_j} (in the associated bundle). The physical flux on the left hand side of (4.29) and the MBQC flux o are off by the simulated U_{total} . By comparing (4.36) with (4.29), we see that U_{total} is analogous to U_{section} in electromagnetism. The analogy is imperfect because U_{total} in MBQC is not associated with one section of the $\mathbb{Z}_2 \times \mathbb{Z}_2$ bundle.

4.4 Elements of computation

4.4.1 Output

We have the following result:

Theorem 2. *For MBQC on 1D cluster states, in all gauges reachable from $\mathbf{f} = 0$ by a gauge transformation, the MBQC output o equals the holonomy g of the MBQC gauge potential \mathbf{g} .*

Proof of Theorem 2. The classical side processing relation (4.7) provides $o = g$, by Theorem 1 valid for all gauges \mathbf{f} equivalent to 0 up to gauge transformation. Then, g has been shown to be the holonomy of the gauge potential \mathbf{g} in Section 4.2.2. \square

³When the gauge group is continuous—like $U(1)$ —the gauge potential is valued in the Lie algebra and its exponentials are group elements. When the gauge group is discrete, we work directly with group elements. Therefore, it is more accurate to say that measurement outcomes g_j are analogous to path-ordered exponentials of $A_\mu dx^\mu$, i.e. Wilson lines of the continuum theory.

The classical side processing relations are, from the phenomenological perspective, an essential ingredient of MBQCs. Even the simplest MBQC—the three-qubit GHZ-MBQC of Anders and Browne [47], repurposing Mermin’s star [46]—has them. Their presence is a direct consequence of the fundamental randomness in quantum measurement. In MBQC, such randomness must be prevented from affecting the logical processing, and the classical side processing relations ensure that. Theorem 2 places the classical side processing relation Eq. (4.7) in the general theoretical framework of gauge theory.

4.4.2 Measurement basis from gauge fixing

In Section 4.1, we explained that changing the reference \mathbf{f} —a choice of one intended gate U_i from the set $[U_i]$ at every i —does not affect an MBQC computation. For this reason, we identified the reference \mathbf{f} with the concept of a section or—in common physics parlance—with the choice of gauge. The reference \mathbf{f} is physically undetectable.

As is common in gauge theory, we can exploit the flexibility in choosing \mathbf{f} for our convenience by imposing suitable gauge-fixing conditions. A particularly convenient gauge-fixing condition reads:

$$V_{g_i} = 1 \quad \text{for all } i < N \quad (4.37)$$

Note that the condition is imposed on all blocks except the final one. We cannot impose $V_g = 1$ on *all* blocks because, by equation (4.27), this would incorrectly reset the physical flux of the resource state.⁴ Gauge condition (4.37) has no independent meaning before a run of MBQC is executed. The choice of reference that is consistent with (4.37) depends on the registered measurement outcomes. More explicitly, up to (but excluding) the final block, the condition demands that the section value f_i on the i^{th} block be simply equal to the outcome of the i^{th} measurement. Equating the reference with the measurement outcome locally obviates the need for a byproduct, thereby setting $V_{g_i} = 1$.

On the final block, the reference can be chosen so that:

$$\prod_i U_{f_i} = U_{\text{total}} \quad (4.38)$$

We have seen in equation (2.23) that a complete run of MBQC induces a transformation in virtual space, which equals BU_{total} , where B is the byproduct operator. A gauge fixing choice, which best accords with the MBQC interpretation, will pick a section which—if measured—ends up simulating U_{total} with no need for further corrections.

The adaptive gauge selects the measurement basis An obvious feature of the adaptive gauge is that the measurement basis executed in an MBQC run must always include the section value f_i , for all i . After all, on each block $i < N$, the section f_i equals the measured basis state. On the final block, the measurement basis certainly contains the state, which

⁴In the continuum, this corresponds to the fact that the gauge potential can always be locally set to zero, but a nonvanishing flux represents an obstruction to achieving such a gauge globally.

induces U_{total} as the transformation on virtual space. That state completes the choice of the adaptive gauge according to equation (4.38).

In summary, the fiber element f_i that is selected by the adaptive gauge-fixing condition stands for a state, which must necessarily be part of the measurement basis on block i . The full measurement basis over block i is the $\mathbb{Z}_2 \times \mathbb{Z}_2$ multiplet, which is generated from $|f_i\rangle$ by the projective representation $l(g)$. We saw this measurement basis multiplet explicitly in equation (3.12). The section $|f_i\rangle$, from which the multiplet is generated, is the reference state (3.11).

We emphasize that identifying a section f_i with the measurement record on $i < N$ —and with the adaptive measurement basis everywhere—is a gauge choice, not an identity. Other gauge choices are viable, and indeed necessary, for defining MBQC. When planning an MBQC calculation, a quantum programmer must select a set of reference angles α_i , which will be subject to later adaptation. At this initial planning stage (sometimes called pre-compiling), the programmer does not yet know the outcomes of future measurements and so cannot gauge-fix according to (4.37). Pre-compiling crucially requires gauges other than (4.37).

MBQC measurement gauge and temporal order The relation between the MBQC measurement basis and the reference in the adaptive gauge—the fact that the former always contains the latter—gives an explanation for the temporal order in MBQC. Condition $V_g = 1$ (or any other gauge condition) can only be imposed by acting with $r(g) \otimes l(g)$ because those are the generators of gauge transformations (4.12). The action of $l(g)$ fixes $V_g = 1$, but the associated action of $r(g)$ always affects the section on the subsequent site. Since equation (4.37) identifies the section with the measurement basis, this is synonymous with the adaptation of the MBQC measurement basis.

Of course, condition (4.37) can only be applied in a temporally ordered fashion. This is evident from the mechanics of MBQC, but the gauge theory language reveals a deeper explanation. The condition $V_{g_i} = 1$ sets Wilson lines $V_{g_{\prec j}} \equiv 1$ for all $1 \leq j \leq N$. (This includes the gauge-fixing condition (4.38) because $V_{g_{\prec N}} = B$.) Those Wilson lines are path-ordered products of individual V_{g_j} s. Setting $V_{g_{\prec j}} \equiv 1$ can only be done in a time-ordered fashion: first $V_{g_{\prec 1}} \equiv V_{g_1}$, then $V_{g_{\prec 2}} \equiv V_{g_2} V_{g_1}$, etc.

5 Phenomenological ramifications of the gauge principle

5.1 Equivalent measurement records

As reviewed in Section 2, there are classes of distinct measurement records that yield the same computational output. This is reflected in the classical side processing relations. Here we show how the MBQC gauge transformations, together with the MPS tensor symmetry $l(\mathbb{Z}_2 \times \mathbb{Z}_2)$, imply this property. Specifically, we show that the change in the measurement record $\mathbf{g} = (g_1, g_2, \dots, g_N)$ given by

$$\mathbf{g} \rightarrow (g_1, \dots, g_{i-1}, h^{-1}g_i, hg_{i+1}, g_{i+2}, \dots, g_N) \quad (5.1)$$

leaves the circuit simulation invariant for all $h \in \mathbb{Z}_2 \times \mathbb{Z}_2$. These transformations, with h acting on all adjacent block pairs except $(N, 1)$, generate a class of equivalent outcomes.

To show this, we subject the product $A_{\mathbf{g}, \mathbf{f}}$ to the MBQC gauge transformation (4.3) and (4.11). Only the product $A_{g_{i+1}, f_{i+1}} A_{g_i, f_i}$ is potentially non-trivially affected, and so we focus on that part:

$$\begin{aligned}
A_{g_{i+1}, f_{i+1}} A_{g_i, f_i} &= \left(V_{g_{\prec i+1}} (V_{g_{i+1}} U_{f_{i+1}}) V_{g_{\prec i+1}}^\dagger \right) \left(V_{g_{\prec i}} (V_{g_i} U_{f_i}) V_{g_{\prec i}}^\dagger \right) \\
&\mapsto \left(V_{\tilde{g}_{\prec i+1}} \left(V_{\tilde{g}_{i+1}} U_{\tilde{f}_{i+1}} \right) V_{\tilde{g}_{\prec i+1}}^\dagger \right) \left(V_{\tilde{g}_{\prec i}} \left(V_{\tilde{g}_i} U_{\tilde{f}_i} \right) V_{\tilde{g}_{\prec i}}^\dagger \right) \\
&\propto \left(V_{\tilde{g}_{\prec i+1}} \left(V_{g_{i+1}} V_h U_{f_{i+1}} V_h^\dagger \right) V_{\tilde{g}_{\prec i+1}}^\dagger \right) \left(V_{\tilde{g}_{\prec i}} (V_{g_i} U_{f_i}) V_{\tilde{g}_{\prec i}}^\dagger \right) \\
&\propto \left(V_{\tilde{g}_{\prec i+1}} (V_h (V_{g_{i+1}} U_{f_{i+1}})) V_{\tilde{g}_{\prec i+1}}^\dagger \right) \left(V_{\tilde{g}_{\prec i}} (V_h^\dagger (V_{g_i} U_{f_i})) V_{\tilde{g}_{\prec i}}^\dagger \right) \\
&= \left(V_{\tilde{g}_{\prec i+1}} V_h g_{i+1} U_{f_{i+1}} V_{\tilde{g}_{\prec i+1}}^\dagger \right) \left(V_{\tilde{g}_{\prec i}} V_{h^{-1} g_i} U_{f_i} V_{\tilde{g}_{\prec i}}^\dagger \right) \\
&= A_{h g_{i+1}, f_{i+1}} A_{h^{-1} g_i, f_i}
\end{aligned}$$

In the second line we applied the gauge transformation $h^{(i)}$ according to eq. (4.11), in the third line we unravelled it, in the fourth line we reordered operators that commute up to phase. In the fifth line and the sixth line, we used the left symmetry $l(h)$ and noted that adaptation in the $i+1$ block given by the conjugation of $V_{\tilde{g}_{\prec i}}$ is consistent with the change in measurement outcome $g_i \rightarrow h^{-1} g_i$ on the previous block.

Thus we have shown that measurement records related by

$$\begin{aligned}
g_{i+1} &\rightarrow h g_{i+1}, & g_i &\rightarrow h^{-1} g_i \\
f_{i+1} &\rightarrow f_{i+1} & f_i &\rightarrow f_i
\end{aligned} \tag{5.2}$$

are equivalent with respect to the quantum computation. We emphasize that unlike the gauge transformations, in (5.2) the group labels change while the references are fixed. Consequently, the gauge invariant outcomes $s_i = g_i f_i$ transform as

$$s_i \rightarrow h^{-1} s_i, \quad s_{i+1} \rightarrow h s_{i+1}, \tag{5.3}$$

whereas all other measurement outcomes remain unchanged.

5.2 MBQC holonomy and the virtual circuit simulation

For simplicity, here and in the next subsection we consider the special case of deterministic MBQC, i.e., where one of the four possible output values o occurs with unit probability. This means that

$$U_{\mathbf{f}} \in [I].$$

Note that this does not require that all local measurement bases are the trivial X -basis. The Pauli unitary $U_{\mathbf{f}}$ may be accumulated in small (non-Clifford) chunks.

The cluster state resolved in the measurement basis is:

$$|1\rangle = \mathcal{N} \sum_{\mathbf{g}} \text{Tr}(A_{\mathbf{g},\mathbf{f}}) |\mathbf{g}, \mathbf{f}\rangle.$$

With eq. (4.9) and the case assumption $U_{\mathbf{f}} \in [I]$, it holds that $A_{\mathbf{g},\mathbf{f}} \in [I]$, for all (potential) measurement records \mathbf{g} . Therefore, for all measurement records \mathbf{g} that can actually occur with non-zero probability, it follows that $A_{\mathbf{g},\mathbf{f}} = I$. Using (4.9) again, we find that

$$U_{\mathbf{f}} = V_o^{-1} \propto V_o, \quad (5.4)$$

for all measurement records that occur with non-zero probability. Thus, the holonomy $U_{\mathbf{f}}$ of the virtual quantum register is cancelled by the holonomy $o = g$ of the gauge potential \mathbf{g} . This goes to the essence of the MPS circuit model interpretation [20] of MBQC: the circuit model quantum register, living on the virtual (or correlation) space, is never directly probed. It interacts with the physical spins, and those are being measured. The measurement record gives rise to the holonomy g , which equals the MBQC output. Thus, the virtual quantum register is measured indirectly, relying on the above cancellation of holonomies.

Non-deterministic simulations require a more detailed analysis, which involves quantum superpositions of fluxes. That case will be covered in Section 5.4.

5.3 Computational output and homotopy

Here we introduce the notion of MBQC order parameter, and discuss how the non-Abellianness of the first homotopy group of the order parameter space relates to MBQC temporal order.

We observed in (4.1) that in the MBQC implementation of every gate U_i we can only aim for the equivalence class $[U_i]$. This suggests that it is meaningful to consider $[U_{\prec t}]$ as an order parameter, evolving in time t . The possible order parameters form the manifold \mathcal{M} .

With an eye on homotopy, we want the time parameter to be continuous. This is achieved as follows: for an integer time i , $i \leq t \leq i+1$, the measurement angles $\alpha_{i,1}$ and $\alpha_{i,2}$ are ramped up continuously from $\alpha_{i,1} = \alpha_{i,2} = 0$ to their intended values as t increases from i to $i+1$. In this way, we are mapping the interval $[0, N] \ni t$ to a trajectory in the parameter space \mathcal{M} . In our MBQC on a cluster ring, this parameter space is

$$\mathcal{M} = SU(2)/\mathcal{Q}. \quad (5.5)$$

Herein $\mathcal{Q} = \{\pm I, \pm iX, \pm iY, \pm iZ\}$ is the quaternion group, which is the lift of the group $\mathbb{Z}_2 \times \mathbb{Z}_2$ into $SU(2)$.

For deterministic MBQCs, $[U_{\prec t}]$ is the same at $t = 0$ and $t = 2$. We may therefore identify the two points, and obtain a mapping from the circle into \mathcal{M} . These maps, with base point at $t = 0$, are classified by the first homotopy group $\pi_1(\mathcal{M})$. They are also classified by the total (Pauli) unitary accumulated in $U_{\prec N} \in SU(2)$ at time $t = N$, and it is the same classification.

For our order parameter space of eq. (5.5), the first homotopy group is:

$$\pi_1(SU(2)/\mathcal{Q}) = \mathcal{Q}. \quad (5.6)$$

The total Pauli operator accumulated during the evolution from continuous time $t = 0$ to $t = N$ is not visible in \mathcal{M} at any given instant of time, because its modded out in \mathcal{M} . But it is captured in the trajectory in \mathcal{M} as a whole, specifically as the homotopy class of the trajectory.

We learn: In case of deterministic MBQC, the total unitary accumulated is an element of the homotopy group $\pi_1(\mathcal{M})$. This group element contains the computational output o , and in addition a global phase ± 1 .

The phase ± 1 shows up in the classification but is not directly of physical interest. So one may wonder whether it is a nuisance or a feature. There is indeed a role that the phases play—they are a signature of the non-Abelianness of the homotopy group \mathcal{Q} . Is the non-Abelianness of \mathcal{Q} of significance for MBQC?

The elements of \mathcal{Q} are the byproduct operators, which are also the generators of the simulated unitary evolution. We recall that the forward-propagation of byproduct operators is responsible for temporal order in MBQC. And this is precisely where the commutation relations of the byproduct operators come into play. There is non-trivial temporal order if and only if the byproduct operators do not commute.

Analogy. A system from classical physics with the same order parameter space $\mathcal{M} = SO(3)/(\mathbb{Z}_2 \times \mathbb{Z}_2) = SU(2)/\mathcal{Q}$ are the biaxial nematics [48]. There, too, the non-Abelianness of $\pi_1(\mathcal{M})$ matters. Namely, it gives rise to non-trivial interaction among linear defects in 3D crystals of such materials. See Fig. 12 for a comparison of the two realizations of the order parameter space.

5.4 A quantum MBQC gauge theory

A classical gauge theory is described by a principal fiber bundle on which every path γ in the base space picks out a definite holonomy. In contrast, a quantum gauge theory accommodates (and requires) superposition of states with different holonomies. For example, such superpositions are a basic feature of quantum electrodynamics, in which Wilson loops are fluctuating observables.

Likewise, in MBQC, holonomies are superposed in order to simulate a general unitary $U \in SU(2)$ in a probabilistic fashion. More precisely, given an expansion

$$U = \sum_o c_o V_o, \quad o \in \mathbb{Z}_2 \otimes \mathbb{Z}_2 \quad (5.7)$$

the cluster state can be expanded in terms of a set of U -dependent, entangled states $|U^\dagger V_o\rangle$

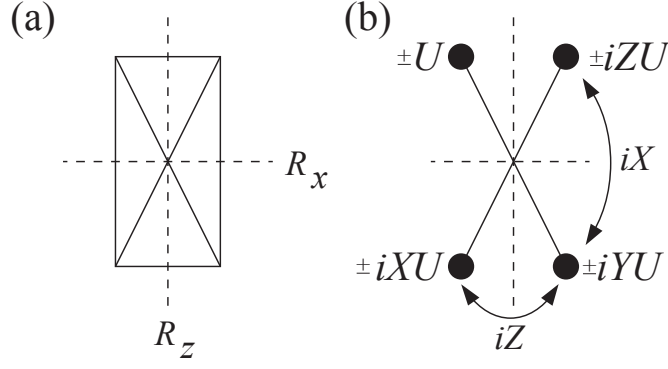


Figure 12: The order parameter spaces for biaxial nematics and MBQC on a cluster ring are the same, $\mathcal{M} = SO(3)/(\mathbb{Z}_2 \times \mathbb{Z}_2) = SU(2)/\mathcal{Q}$. (a) Order parameter of biaxial nematics. The symmetry is realized by reflections about the horizontal and the vertical axis. (b) Order parameter of MBQC on a cluster ring. The symmetry is implemented by left-multiplication with elements of \mathcal{Q} .

with holonomy o :

$$|1\rangle = \sum_o c_o |U^\dagger V_o\rangle \quad (5.8)$$

Equations (5.7) and (5.8) generalize the relation (5.4) between o and the U to allow for quantum superpositions. The probabilities $|c_o|^2$ provide a sort of state-operator correspondence, in which logical states $|U^\dagger V_o\rangle$ in the physical Hilbert space are mapped to operators U in the virtual space.⁵ In this section, we explain the precise nature of this correspondence. In particular, we will show how the logical states $|U^\dagger V_o\rangle$ arise from a decomposition of the physical Hilbert space into flux sectors, and how MBQC uses this decomposition to implement quantum computations.

5.4.1 Superselection (flux) sectors

Superselection sectors in the X -basis In Section 2 we showed that the holonomy o is invariant under changes of the measurement record generated by stabilizers. These transformations permute the computationally equivalent measurement outcomes described in Section 5.1. They determine a basis, which forms an orbit under the action of the stabilizers

$$\mathcal{L} = \{K_i, i = 2, \dots, N-1\}. \quad (5.9)$$

⁵Actually MBQC only determines the modulus of c_o and not the relative phases. This feature is explained below in terms of the decomposition of the Hilbert space into superselection sectors.

We exclude the stabilizers K_1 and K_N because they are not needed to span the measurement outcomes, and are also inconsistent with the temporal order on the circle.⁶

We define a flux sector to be the span of such an orbit. Each flux sector is labelled by the holonomy o , so that the total Hilbert space \mathcal{H}_{S^1} on a circle decomposes into a direct sum

$$\mathcal{H}_{S^1} = \oplus_o \mathcal{H}_o \quad (5.10)$$

As an example, for measurements along X , the basis for \mathcal{H}_o comprises X -eigenstates:

$$|g_{2N}\rangle \otimes \dots \otimes |g_1\rangle, \quad o = \prod_i g_i \quad (5.11)$$

We first encountered these sectors in Section 2.1, in the paragraph ‘A glimpse of a global structure.’

Twisted states We continue to concentrate on X -measurements, postponing the general case till the next paragraph. In each sector labeled by $o \in \mathbb{Z}_2 \times \mathbb{Z}_2$, there is a distinguished representative, which can be expressed as an entangled matrix product state:

$$|V_o\rangle := \mathcal{N} \sum_{g_j \in \mathbb{Z}_2 \times \mathbb{Z}_2} \text{Tr}(V_o A_{g_N} \dots A_{g_2} A_{g_1}) |g_N\rangle \dots |g_2\rangle |g_1\rangle. \quad (5.12)$$

Notice that the cluster state, as defined in (2.5), is (5.12) with $V_o = 1$. This is the precise reason for denoting the cluster state as $|1\rangle$.

Equation (5.12) encompasses three other matrix product states— $|X\rangle$, $|Z\rangle$, and $|XZ\rangle$ —which are canonical representatives of the three other superselection sectors. Their wavefunctions overlap only with those states $|g_N\rangle \dots |g_2\rangle |g_1\rangle$ whose labels satisfy

$$g_N \dots g_2 g_1 = o. \quad (5.13)$$

Notice that any of these states can be used as a resource for MBQC. In particular, measurements of $|V_o\rangle$ along X give the deterministic computational output o .

Including a nontrivial V_o in the wavefunction (5.12) is an insertion of physical $\mathbb{Z}_2 \times \mathbb{Z}_2$ flux. We will call states $|V_o\rangle$ ‘twisted states’ because a flux insertion corresponds to imposing a ‘twisted boundary condition’ on a matter particle living in virtual space. In a continuum gauge theory, such twisted boundary conditions are implemented by coupling a matter field $\Phi(x)$ to the gauge field via $\Phi(x) \rightarrow e^{i \oint^x A_\mu dx^\mu} \Phi(x)$ and demanding:

$$\Phi(x + 2\pi) = e^{i \oint^A} \Phi(x) \quad (5.14)$$

⁶The temporal order in MBQC selects out a ‘base point’ on the circle, which separates the past from the future. Indeed, measurement outcomes at the $j = N$ block should not affect measurement angles at the $j=1$. The stabilizers K_1, K_N violate this constraint.

Flux sectors for a general measurement basis We can apply the same logic to decompose \mathcal{H}_{S^1} into sectors $\mathcal{H}_o(U)$ defined with respect to a general, U -dependent measurement basis:

$$\bigotimes_{j=1}^{2N} |(-)^{s_j}_{((-)^{q_j} \alpha_j)}\rangle = \bigotimes_{i=1}^N |g_i\rangle \quad (5.15)$$

A projection of the cluster state onto a product state in (5.15) represents one measurement history of an MBQC computation, which is designed to simulate a unitary U . These histories, too, fall into four orbits under \mathcal{L} . Each orbit is labeled by the holonomy $o = \prod_i g_i$, where the group labels $g_i \in \mathbb{Z}_2 \times \mathbb{Z}_2$ are relative to a section in the adapted basis.

Following (5.12), we define twisted matrix product states, which have definite holonomy as measured by a run of MBQC:

$$|U^\dagger V_o\rangle := \mathcal{N} \sum_{g_j \in \mathbb{Z}_2 \times \mathbb{Z}_2} \text{Tr}(U^\dagger V_o A_{g_N} \dots A_{g_2} A_{g_1}) |g_N\rangle \dots |g_2\rangle |g_1\rangle \quad (5.16)$$

Note that this notation is consistent with the definition in (5.12) because the combination

$$\sum_{g_j \in \mathbb{Z}_2 \times \mathbb{Z}_2} (A_{g_N} \dots A_{g_2} A_{g_1}) |g_N\rangle \dots |g_2\rangle |g_1\rangle \quad (5.17)$$

is basis-independent. So equation (5.16) can be read with $|g\rangle$ defined relative to any measurement basis. In particular, for measurements in the X -basis, the twisted states (5.16) reduce to equation (5.12) with V_o replaced by $U^\dagger V_o$.

The twisted states (5.16) can be characterized by the fact that running an MBQC simulation of U on them would return a deterministic outcome. Indeed, using (2.23), we can express the wavefunction of these twisted states in the adapted basis as:

$$\text{Tr}(U^\dagger V_o A_{g_N} \dots A_{g_2} A_{g_1}) = \text{Tr}(V_o B_{g_N \dots g_2 g_1}) \propto \delta_{o, g_N \dots g_2 g_1} \quad (5.18)$$

Thus, state $|U^\dagger V_o\rangle$ has definite MBQC holonomy $o = g_N \dots g_2 g_1$.

5.4.2 A logical Hilbert space of fluxes

The resource states for MBQC live in the 2^{2N} -dimensional Hilbert space \mathcal{H}_{S^1} of physical qubits. On the other hand, the twisted states span a four-dimensional Hilbert space

$$\mathcal{H}_{\text{flux}} = \text{span}\{|V_o\rangle\} \quad (5.19)$$

whose kets represent flux sectors of the gauge theory. MBQC uses $\mathcal{H}_{\text{flux}}$ as a logical Hilbert space to perform quantum computations. In particular, MBQC makes use of the freedom to rotate the basis of twisted states (5.12) into (5.16). We can make the unitary rotation explicit

by reading both (5.12) and (5.16) in the X -basis, and then expanding:

$$U^\dagger := \sum_{k \in \mathbb{Z}_2 \times \mathbb{Z}_2} \tilde{c}_k V_k \quad (5.20)$$

The linearity of the matrix product states then immediately implies:

$$|U^\dagger V_o\rangle = \mathcal{N} \sum_{k \in \mathbb{Z}_2 \times \mathbb{Z}_2} \tilde{c}_k \sum_{g_j \in \mathbb{Z}_2 \times \mathbb{Z}_2} \text{Tr}(V_k V_o A_{g_N} \dots A_{g_2} A_{g_1}) |g_N\rangle \dots |g_2\rangle |g_1\rangle = \mathcal{N} \sum_k \tilde{c}_k b(k, o) |V_{ko}\rangle, \quad (5.21)$$

where $b(k, o)$ is the projective phase defined by $V_k V_o = b(k, o) V_{ko}$.

We thus have two flux bases for $\mathcal{H}_{\text{flux}}$. On the one hand, we have a canonical set $|V_o\rangle$ to which the cluster state $|1\rangle$ belongs; these are resource states that an MBQC technician will hold in her lab. On the other hand, we have $|U^\dagger V_o\rangle$, defined so that a U -simulating MBQC protocol conducted on the initial state $|U^\dagger V_o\rangle$ would return a definite holonomy (deterministic computational output.) While the latter are not resource states, they are nevertheless essential in MBQC.

To see this, let us revisit the MBQC protocol on a ring from the perspective of $\mathcal{H}_{\text{flux}}$. We can expand the cluster state $|1\rangle$ in terms of $|U^\dagger V_o\rangle$ by applying the inverse of (5.21), or equivalently, by expanding $U = \sum_o c_o V_o$ in equation (3.20). This gives:

$$\begin{aligned} \mathcal{N}^{-1} |1\rangle &= \sum_g \text{Tr}(U B_{g_N \dots g_2 g_1}) |g_N\rangle \dots |g_2\rangle |g_1\rangle \\ &= \sum_o c_o \left(\sum_g \text{Tr}(V_o B_{g_N \dots g_2 g_1}) |g_N\rangle \dots |g_2\rangle |g_1\rangle \right) \\ &= \sum_o c_o |U^\dagger V_o\rangle \end{aligned} \quad (5.22)$$

Recall from Section 3.3 that the raw output of an MBQC calculation on a ring is a probability distribution $p_o = |c_o|^2$, which characterizes the simulated unitary U . Thus, even though MBQC is physically implemented by single qubit measurements, from a global perspective it is measuring the MBQC flux corresponding to $|U^\dagger V_o\rangle$.

5.4.3 MBQC versus the circuit model

Equation (5.22) presents the cluster state as an element of the four-dimensional flux Hilbert space $\mathcal{H}_{\text{flux}}$. This perspective provides an important insight into the relation between MBQC and the circuit model. To illustrate this relation, consider the following hypothetical realization of the circuit model. Suppose we can create arbitrary superpositions of the twisted states $|V_o\rangle$. We could then effectively apply a unitary rotation on $\mathcal{H}_{\text{flux}}$ such that

$$|1\rangle \rightarrow |U\rangle = \sum_o c_o |V_o\rangle \quad (5.23)$$

In the X -basis, the resulting resource state is:

$$|U\rangle = \mathcal{N} \sum_{g_1, \dots, g_n} \text{tr}(U A_{g_N} \cdots A_{g_1}) |g_N\rangle \cdots |g_1\rangle \quad (5.24)$$

The form of this MPS wavefunction implies that single qubit measurements of $|U\rangle$ along X will simulate the unitary U . The computational output is

$$p_o = |\langle V_o | U \rangle|^2 = |c_o|^2. \quad (5.25)$$

From the point of view of the flux Hilbert space $\mathcal{H}_{\text{flux}}$, this protocol is a realization of the circuit model.

Let us contrast this with MBQC. Here, too, we start with $|1\rangle$ as the initial state. However, instead of applying unitary gates to $|1\rangle$, we measure it in the basis $|U^\dagger V_o\rangle$. Equation (5.21) implies these measurements produce the same probability distributions as above:

$$p_o = |\langle U^\dagger V_o | 1 \rangle|^2 = |c_o|^2 = |\langle V_o | U \rangle|^2 \quad (5.26)$$

In this way, MBQC can be viewed as a ‘passive’ counterpart to an ‘active’ circuit model. Whereas the circuit model implements its programming via the active transformations $|1\rangle \rightarrow |U\rangle$, MBQC implements its programming via a U -dependent rotation of the measurement basis. In particular, from the viewpoint of the logical Hilbert space $\mathcal{H}_{\text{flux}}$, MBQC measurements project $|1\rangle$ onto the rotated states $|U^\dagger V_o\rangle$. Meanwhile, from the perspective of the physical Hilbert space \mathcal{H}_{S_1} , MBQC projects $|1\rangle$ onto a superselection sector $\mathcal{H}_o(U)$ represented by $|U^\dagger V_o\rangle$. This superselection sector is defined by the U -dependent decomposition

$$\mathcal{H}_{S_1} = \oplus_o \mathcal{H}_o(U), \quad (5.27)$$

which is determined by the change of basis (5.21) from $|V_o\rangle$ to $|U^\dagger V_o\rangle$. This rotation is responsible for introducing temporal order into the measurement basis.

5.5 Extension to fixed point of SPT phases with onsite symmetries

In the preceding sections, we have formulated all elements of the MBQC gauge theory in terms of the symmetry actions $l(g)$, $r(g)$, and $u(g)$, as well as the equivariant transformation laws of the cluster MPS tensor; see Figure 5. These symmetry properties are not unique to the cluster state. Indeed, they are shared by resource states that belong to the fixed point of any SPT phase protected by an onsite symmetry G . Such a resource state has a ‘fixed point’ MPS representation [18], in which G acts via the ordinary representation $u(g)$. As in the cluster state, this symmetry fractionalizes into left and right projective representations $l(g)$ and $r(g)$ in the sense that $u(g) = l(g)r(g)$. Moreover, the fixed point MPS tensor satisfies the same equivariant transformation laws shown in Figure 5. Therefore, we expect that our formulation of the MBQC gauge theory applies to each of these fixed points.

5.6 Extension of the gauge principle to SPT cluster phase

The 1D cluster state is surrounded by an SPT phase with global symmetry $\mathbb{Z}_2 \times \mathbb{Z}_2$ [24–26]. It is known that MBQC computational power extends from the 1D cluster state into all of that phase [27]. What about the MBQC gauge principle—does it extend as well? In this regard, we have the following result:

Theorem 3. *For any given MBQC on a ground state in the $\mathbb{Z}_2 \times \mathbb{Z}_2$ SPT phase surrounding the 1D cluster state, the measurement bases $|g_i, f_i\rangle$ chosen as a function of prior measurement record $g_{<i}$, the output o given the measurement record \mathbf{g} , and the probability distribution of the computational output o , $p(o) = |\text{Tr}(U_{\mathbf{f}}V_o)|^2$, are all invariant under the gauge transformations (4.11-4.13).*

The proof of Theorem 3 is the same as of Theorem 1.

Remark: The reason that the proofs of Theorems 1 and 3 are the same is that both theorems are chiefly about the classical side processing in MBQC (items (i) and (ii)), and this classical side processing extends from the cluster state into the surrounding SPT phase without change [27]. The invariance of $p(o)$ in item (iii) also follows as before, but the equality $p(o) = |\text{Tr}(U_{\mathbf{f}}V_o)|^2$ needs to be established for the SPT phase first; this was done in [27].

There is a lesson to learn from the ease with which the MBQC gauge principle extends from the cluster point into the surrounding phase. The gauge theory of MBQC is, in a certain sense, complementary to ‘computational phases of quantum matter,’ i.e., to viewing MBQC through the lens of symmetry-protected topological order. Computational phases of matter are about quantum states. The MBQC gauge theory is, in turn, about observables.

6 Conclusion

The main thesis of this work is that the workings of MBQC can be recast in terms of concepts from gauge theory. The principal identifications are as follows:

1. There are many ways to describe the same MBQC computation to a lab technician. They are related by gauge transformations; see Section 4.1.
2. Under a suitable gauge-fixing condition (equations 4.37-4.38), different gauges also correspond to distinct but computationally equivalent measurement records. Imposing this gauge-fixing condition determines the temporal order in the adaptation of measurement angles; see Section 4.4.2.
3. Computational output is a holonomy of the gauge field or, equivalently, a flux; see equation (4.32).

We hope that this correspondence helps to bridge a gap between the quantum computing community and high energy and condensed matter theorists, for whom gauge theory is an essential tool. From the condensed matter perspective, a connection between MBQC and

gauge theory could have been anticipated: a large class of MBQC resource states have SPT order [23–31], and SPT order has been characterized in gauge theoretic terms []. In this sense, our work completes the missing link in the triangle: MBQC-SPT-gauge theory.

Several features of the gauge theoretic description of MBQC may seem unfamiliar or even exotic when compared with a standard textbook on gauge theory. The foremost of them is that MBQC encodes the simulated unitary U using linear superpositions of distinct physical fluxes; see equation (5.16). Such flux superpositions give our gauge theory the flexibility to describe all MBQC computations (in one dimension) in one unified language. Different simulated U s lead to distinct notions of MBQC flux, but each of them is unitarily related to physical flux; see equation (4.32).

One innovation, which made our analysis possible, was to consider as resources cluster states with the topology of a circle. On a technical level, this is what allowed us to define fluxes—that is, holonomies of a fiber bundle. But the novelty of considering circular resource states also brings about a modest practical benefit. In contrast to MBQC on a cluster with endpoints, MBQC on a ring-like resource extracts two classical bits $o \in \mathbb{Z}_2 \times \mathbb{Z}_2$ of computational output. This agrees with the common lore (superdense coding) that one qubit is worth two classical bits.

Circular resource states are also intriguing from a more conceptual point of view, which concerns the relationship between gauge theory and teleportation. We have motivated our analysis by explaining that MBQC in one dimension is a sequence of gate teleportations. Our identifications between MBQC and gauge theory concepts therefore have direct meaning in quantum teleportation:

1. Physical parallel transport (4.20) is the gate, which is induced by a projective measurement in quantum gate teleportation.
2. The intended gate in gate teleportation depends on the intention of the sender and recipient, so it is not gauge invariant. Different intended gates correspond to different gauges—different reference states $|f\rangle$ for the projective measurements.
3. The classical information sent by Alice to Bob concerns how the measured state $|g\rangle$ differs from $|f\rangle = l(g)^{-1}|g\rangle$. That is, the classical message exchanged in quantum teleportation is an analogue of the gauge potential.

These identifications extend and complement similar observations about quantum teleportation, which were made in [33]; see also [34]. Ref. [33] argued that quantum teleportation with post-selection has the same physical effect as parallel transport of a charged particle in a background gauge field. This is a special case of our identifications, restricted to the circumstance where no corrective operation is necessary. The present work generalizes [33] by removing the post-selection assumption, and by explaining that the corrective operator applied by Bob (the recipient) plays the role of the gauge connection. It also explains how the ‘entanglement holonomies’ defined in [33] can be constructed and measured in a lab. To close an ‘entanglement holonomy,’ the authors of [33] needed a sequence of teleportations,

with the initial state of the first teleportation identified with the final state of the last one. MBQC can realize this setup without closing a loop in time and without post-selection—by using a resource state with a ring-like topology.

Future directions. This paper covers MBQC on one-dimensional resource states—settings, which afford simulation of single-qubit gates. For universal quantum computation, one also needs an entangling gate. To simulate it, MBQC requires a two-dimensional resource state. Upgrading our discussion to this more elaborate context is the obvious next step of our program.

Another specialization adopted in this paper is that we mostly focused on MBQC on circular resource states. They are best suited for the gauge-theoretic treatment because they naturally support holonomies / fluxes, i.e. Wilson loops. But in its conventional form, MBQC assumes a resource state with the topology of a line segment. Naïvely, designing a gauge-invariant computational output on a line segment is challenging because the natural objects—Wilson lines—are not gauge-invariant. The solution involves Stückelberg fields / edge modes of the gauge theory [1, 2, 51], whose transformations cancel out the gauge dependence of a Wilson line at its endpoints. We postpone a detailed description of conventional MBQC in terms of gauge theory with Stückelberg fields till a future publication.

A different conceptual perspective, which we mentioned only briefly in the current work, would take the symmetry protected topological (SPT) order of the resource state as an analytic starting point. SPT-ordered phases of matter are in one-to-one correspondence [50] with equivariant topological field theories (TFT) [3]. This correspondence suggests elevating the connection between MBQC and gauge theory to one with topological field theory. That, in turn, should bring to focus aspects of MBQC that are more germane to the spirit of a topological field theory, for example scale invariance or an axiomatic definition.

Acknowledgments

GW acknowledges support by Fudan University, the Thousand Talents Program, and Harvard CMSA. RR is supported by NSERC, in part through the Canada First Research Excellence Fund, Quantum Materials and Future Technologies Program, and by US ARO (W911NF2010013). We thank the organizers of workshop ‘Quantum Information and String Theory 2019’ held at Yukawa Institute for Theoretical Physics, Kyoto University, where this work was initiated. We also acknowledge the workshop ‘Symmetry, Phases of Matter and Quantum Computing – ASQC’ (2019) held at Perimeter Institute and BC acknowledges the workshop ‘Reconstructing the Gravitational Hologram with Quantum Information’ (2022) held at the Galileo Galilei Institute in Florence, where this work was partly carried out.

References

- [1] P. V. Buividovich and M. I. Polikarpov, Phys. Lett. B **670**, 141-145 (2008) doi:10.1016/j.physletb.2008.10.032 [arXiv:0806.3376 [hep-th]].

- [2] W. Donnelly, *Class. Quant. Grav.* **31**, no.21, 214003 (2014)
doi:10.1088/0264-9381/31/21/214003 [arXiv:1406.7304 [hep-th]].
- [3] G. W. Moore and G. Segal, [arXiv:hep-th/0609042 [hep-th]].
- [4] R. Raussendorf and H.-J. Briegel, *Phys. Rev. Lett.* **86**, 5188 (2001).
- [5] M. Van den Nest, W. Dür, G. Vidal, H. J. Briegel, *Phys. Rev. A* **75**, 012337 (2007).
- [6] M. Van den Nest, A Miyake, W Dür, HJ Briegel, *Phys. Rev. Lett.* **97**, 150504 (2006).
- [7] D. Gross, S. T. Flammia, and J. Eisert, *Phys. Rev. Lett.* **102**, 190501 (2009).
- [8] H.J. Briegel and R. Raussendorf, *Phys. Rev. Lett.* **86**, 910 (2001).
- [9] I. Affleck, T. Kennedy, E.H. Lieb, and H. Tasaki, *Phys. Rev. Lett.* **59**, 799 (1987).
- [10] I. Affleck, T. Kennedy, E.H. Lieb, and H. Tasaki, *Commun. Math. Phys.* **115**, 477 (1988).
- [11] A. Miyake, *Ann. Phys.* **326**, 1656 (2011).
- [12] T.-C. Wei, I. Affleck, and R. Raussendorf, *Phys. Rev. Lett.* **106**, 070501 (2011).
- [13] A.S. Darmawan, G.K. Brennen, S.D. Bartlett, *New J. Phys.* **14**, 013023 (2012).
- [14] Tzu-Chieh Wei, Robert Raussendorf, *Phys. Rev. A* **92**, 012310 (2015).
- [15] S. Bravyi and R. Raussendorf, *Phys. Rev. A* **76**, 022304 (2007).
- [16] Z.C. Gu and X.G. Wen, *Phys. Rev. B* **80**, 155131 (2009).
- [17] X. Chen, Z.C. Gu, and X.G. Wen, *Phys. Rev. B* **82**, 155138 (2010).
- [18] Norbert Schuch, David Perez-Garcia, and Ignacio Cirac, *Phys. Rev. B* **84**, 165139 (2011).
- [19] X. Chen, Z.C. Gu, Z.X. Liu, X.G. Wen, *Phys. Rev. B* **87**, 155114 (2013).
- [20] D. Gross and J. Eisert, *Phys. Rev. Lett.* **98**, 220503 (2007).
- [21] D.E. Browne, E. Kashefi, M. Mhalla, S. Perdrix, *New J. Phys.* **9**, 250 (2007).
- [22] Robert Raussendorf, Tzu-Chieh Wei, Poya Haghegahdar and Pradeep Sarvepalli, *Electronic Proceedings in Theoretical Computer Science (EPTCS)* **95**, pp. 219-250 (2012).
- [23] A. C. Doherty and S. D. Bartlett, *Phys. Rev. Lett.* **103**, 020506 (2009).
- [24] A. Miyake, *Phys. Rev. Lett.* **105**, 040501 (2010).
- [25] D. V. Else, I. Schwarz, S. D. Bartlett, and A. C. Doherty, *Phys. Rev. Lett.* **108**, 240505 (2012).
- [26] J. Miller and A. Miyake, *Phys. Rev. Lett.* **114**, 120506 (2015).
- [27] R. Raussendorf, D.-S. Wang, A. Prakash, T.-C. Wei, and D. T. Stephen, *Phys. Rev. A* **96**, 012302 (2017).
- [28] R. Raussendorf, C. Okay, D.-S. Wang, D. T. Stephen, and H. P. Nautrup, *Phys. Rev. Lett.* **122**, 090501 (2019).
- [29] T. Devakul and D. J. Williamson, *Phys. Rev. A* **98**, 022332 (2018).
- [30] D.T. Stephen, H. P. Nautrup, J. Bermejo-Vega, J. Eisert, and R. Raussendorf, *Quantum* **3**, 142 (2019).
- [31] A.K. Daniel, R.N. Alexander, A. Miyake, *Quantum* **4**, 228 (2020).

- [32] A.M. Childs, D.W. Leung, M.A. Nielsen, Phys. Rev. A **71**, 032318 (2005).
- [33] B. Czech, L. Lamprou L. Susskind, [arXiv:1807.04276 [hep-th]].
- [34] J. Mielczarek, T. Trześniewski, Phys. Lett. B **810** (2020), 135808.
- [35] X. L. Qi, [arXiv:1309.6282 [hep-th]].
- [36] D. Harlow, JHEP **01** (2016), 122.
- [37] B. Czech, [arXiv:2201.01303 [hep-th]].
- [38] R. B. Laughlin, Phys. Rev. Lett. **50** 1395 (1983).
- [39] J. Fuchs, I. Runkel and C. Schweigert, Nucl. Phys. B **646** (2002), 353-497.
- [40] Raussendorf, J. Harrington, K. Goyal, Ann. Phys. (N.Y.) **321**, 2242 (2006).
- [41] R. Raussendorf and J. Harrington, Phys. Rev. Lett. **98**, 190504 (2007).
- [42] N. Nickerson, H. Bombin, arXiv:1810.09621.
- [43] Sam Roberts, Stephen D. Bartlett, Phys. Rev. X **10**, 031041 (2020).
Quant. Inf. Comp. **6**, 443 (2002).
- [44] D. Gottesman, Proceedings of the XXII International Colloquium on Group Theoretical
Methods in Physics, p. 32-43 (Cambridge, MA, International Press, 1999)
- [45] S. Aaronson, D. Gottesman, Phys. Rev. A **70**, 052328 (2004).
- [46] N.D. Mermin, Rev. Mod. Phys. **65**, 803 (1993).
- [47] J. Anders and D.E. Browne, Phys. Rev. Lett. **102**, 050502 (2009).
- [48] N.D. Mermin, Rev. Mod. Phys. **51**, 591 (1979).
- [49] D. Pérez-García and M. M. Wolf and M. Sanz and F. Verstraete and J. I. Cirac, Phys. Rev.
Lett. **100** (2008).
- [50] K. Shiozaki and S. Ryu, JHEP **04**, 100 (2017) doi:10.1007/JHEP04(2017)100 [arXiv:1607.06504
[cond-mat.str-el]].
- [51] W. Donnelly and L. Freidel, JHEP **09**, 102 (2016) doi:10.1007/JHEP09(2016)102
[arXiv:1601.04744 [hep-th]].